An updated empirical correlation formalism for laminar flame speeds : Application to a TRFE gasoline surrogate in highly diluted conditions

Boyang Xu, Pascal Diévart, Mickaël Matrat, Julian Garrec, Laurent Catoire

An Updated Empirical Correlation Formalism for Laminar Flame Speeds: Application to a TRFE Gasoline Surrogate in Highly Diluted Conditions

Boyang Xu[a,b,*], Pascal Diévart[b], Mickaël Matrat[a], Julian Garrec[b], Laurent Catoire[b]

[a] *IFP Energies nouvelles, 1 et 4 avenue de Bois-Préau, 92852 Rueil-Malmaison, France ; Institut Carnot IFPEN Transports Energie*

[b] *Unité Chimie et Procédés, ENSTA Paris, Institut Polytechnique de Paris, 91120 Palaiseau, France*

Abstract

In order to comply with present and future stringent environmental policies, engine manufacturers have to improve engine design and control to achieve combustion with high dilution ratios. The use of CFD simulations with complex combustion chemistry remains prohibitive, and alternatives to assess quickly the laminar flame speeds at local grid cell conditions (temperature, pressure, equivalence ratio, and dilution ratio) are desired, such as empirical correlations. Whereas these correlations should ideally be obtained from experimental measurements, comprehensively validated kinetic models can help extend databases to conditions that cannot be achieved practically. Hence, the present study proposed a reduced kinetic mechanism, containing 593 species and 3698 reactions, for one gasoline surrogate, namely Toluene Reference Fuel with Ethanol addition (TRFE). It is obtained by first compiling sub-mechanisms from the literature for the four components (isooctane, n-heptane, toluene, and ethanol) with updates of some key rate constants, and then is reduced for 1-D flame speed computations. The model was first validated against recent experimental laminar flame speed measurements of TRFE/air/diluent mixtures for various temperatures, pressures, equivalence ratios, and dilution ratios and then employed to extend the experimental database for the TRFE surrogate to higher dilution ratios and temperatures. A new formalism, including new mathematical expressions for the reference and dilution terms, and the temperature exponent are proposed. This new formalism exhibits improved abilites in fitting the laminar flame speeds, especially at high dilution ratios and in very fuel-lean

and fuel-rich conditions. A new mathematical correlation based on these formulas was developed, whose correlation parameters were obtained by fitting both experimental data and mechanism predictions. Regardless of the conditions, the present correlation is observed to show overall good agreements with available experimental data in the literature for laminar flame speeds and their dependence on equivalence ratio, temperature, pressure, and dilution. Results show that the effect of dilution in reducing flame speeds is not linear and depends on the equivalence ratio. A parameter μ is defined in the correlation formulas to evaluate the dilution effectiveness of the diluent, which is found to be composition-specific and possibly follows a linear mixing rule for diluent mixtures.

Keywords:

laminar flame speed, gasoline surrogate, empirical correlation, dilution, exhaust gas recirculation, kinetic mechanism

---

*Corresponding author

Email addresses: boyang.xu@ifpen.fr (Boyang Xu), boyang.xu@outlook.com (Boyang Xu)

Nomenclature

α	Temperature exponent
β	Pressure exponent
γ	Oxygen ratio exponent
μ	Dilution effectiveness
μ_α	Temperature exponent for dilution effectiveness
μ_β	Pressure exponent for dilution effectiveness
μ_i	Dilution effectiveness for individual components in the diluent mixture
μ_{mix}	Dilution effectiveness for the diluent mixture
ν_{O_2}	Oxygen ratio in the non-fuel fraction of the mixture
ρ	Density
v	liquid volume fraction of ethanol in fuel
φ	Equivalence ratio
φ_α	Median equivalence ratio for temperature exponent
φ_β	Median equivalence ratio for pressure exponent
φ_μ	Median equivalence ratio for dilution effectiveness
φ_m	Median equivalence ratio
n_{O_2}	amount of oxygen molecules in moles
P	Pressure
P_i	Initial pressure

P_{ref} Reference pressure

R^2 Coefficient of Determination

$S_{L,max}$ Maximum laminar flame speed

$S_{L,ref}$ Refernce laminar flame speed

T Temperature

T_i Initial temperature

T_{ref} Reference temperature

X_{air} Mole fraction of air in the mixture

X_{EGR} Mole fraction of EGR in the mixture

X_{fuel} Mole fraction of fuel in the mixture

x_d Dilution ratio

X_i Mole fraction

X_{et} Mole fraction of ethanol in fuel

S_L Laminar flame speed

CFD Computational Fluid Dynamics

CURV Adaptive Grid Control Based On Solution Curvature

DRGEP Direct Relation Graph method with Error Propagation

EGR Exhaust Gas Recirculation

FSSA Full Species Sensitivity Analysis

GRAD Adaptive Grid Control Based On Solution Gradient

HCs Unburnt Hydrocarbons

MON Motor Octane Number

NOx Nitrogen Oxides

p.w. Present Work

RMSE Root Mean Squared Error

RON Research Octane Number

SA Sensitivity Analysis

SI Spark Ignition

TRF Primary Reference Fuel

TRF Toluene Reference Fuel

TRFE Toluene Reference Fuel with Ethanol addition

1. Introduction

Engine manufacturers have to comply with more and more stringent environmental public policies, thus pressing to reduce both pollutants emissions (CO, NOx, HCs) and fuel consumption. Over the last decades, Exhaust Gas Recirculation (EGR), as a mean to achieve diluted combustion, has been a technology that benefited Spark Ignition (SI) engines since it has been demonstrated to reduce knock tendency, mitigate NOx emission while promoting fuel savings. [1–5] However, engine operation in highly-diluted regimes (EGR ratio greater than 25%) remains difficult mainly because of the slower heat release rate and the deteriorated engine stability induced. [6] These issues could not be overcome by the measures that proved efficient at lower dilution ratios such as increasing turbulence level and advanced spark-ignition technologies (including increasing ignition energy).[6] In order to propose and develop new strategies to control the combustion at these higher dilution rates, extensive use of turbulent Computational Flow Dynamic (CFD) is required. These CFD codes are based on the flamelets regime assumption, in which the laminar flame speed (S_L) at the grid-cell local conditions (temperature, pressure, equivalence ratio, dilution ratio) is the fundamental property to be determined, explaining the reason why laminar flame speeds measurements are still of great interest. [7] Although kinetic models can be embedded into CFD codes to determine on-the-fly S_L, this approach is limited to small mechanisms (usually less than 50 species) which are challenging to develop with sufficient accuracy for complex fuels. [8] Hence, other strategies have been devised such as empirical correlations.

The commonly used mathematical correlation relates the laminar flame speeds to the equivalence ratio, temperature and pressure, $S_L = f(\varphi, T, P)$.

$$S_L = S_{L,ref}(\varphi)\left(\frac{T}{T_{ref}}\right)^{\alpha}\left(\frac{P}{P_{ref}}\right)^{\beta} \tag{1}$$

where $S_{L,ref}(\varphi)$, the flame speed at a reference condition (T_{ref}, P_{ref}), is a quadratic function of the equivalence ratio, and the exponent α and β are usually linear functions of the equivalence ratio.

With the development of EGR technologies, the necessity to consider the effect of the EGR dilution ratio (x_d) and composition led to the introduction of a corrective term $f(x_d)$.

Early studies by Ryan and Lestz [9], Metghalchi and Keck [10], Gülder [11, 12] reported laminar flame speeds of both single-component fuels and commercial gasoline at various temperatures, pressures, and dilution ratios. The three studies used a synthetic N_2/CO_2 blend (85%/15% by volume, with small variations between the three studies) as the diluent since it has heat capacities similar to the exhaust gas. They observed that, within their investigation range (up to 30% dilution), S_L decreases linearly with the dilution ratio and the decay rate was independent of the unburnt gas temperature. Kumar *et al.* [13] drew the same conclusion by investigating isooctane/air and n-heptane/air flames diluted in N_2. Therefore, the first attempts [9–12] to model the dilution factor adopted a linear expression,

$$f_1(x_d) = 1 - ax_d \tag{2}$$

in which the parameter a was found to lie within 2.1 and 2.5.

Rhodes and Keck [14] measured the propagation speed of spherically expanding flames of two multicomponent gasoline surrogates, with and without prior dilution in a synthetic EGR (N_2/CO_2 = 80%/20% by volume). Unlike previous studies, the dilution effect was observed to be not linear, and the authors thus introduced an exponent on the dilution ratio

$$f_2(x_d) = 1 - ax_d^b \tag{3}$$

and determined a and b to be equal to 2.06 and 0.77, respectively, for both fuels investigated.

As an alternative to experimental measurements, Syed *et al.* [15] carried out a modeling study in which the effect of ethanol blending and EGR dilution on the propagation of gasoline/air flames was investigated. In line with the conclusions of Rhodes and Keck, the simulated data revealed a non-linear dependence on the dilution ratio, which was best captured by the following expression

$$f_3(x_d) = (1 - ax_d)^b \tag{4}$$

where the two coefficients a and b vary slightly with the ethanol fraction.

Bhattacharya *et al.* [16] measured using the heat-flux burner technique the atmospheric laminar flame speeds of gasoline/air mixtures diluted in up to 15% of N_2. They observed that

the laminar flame speed decrease caused by the N_2 dilution was equivalence ratio dependent, and thus adopted for the dilution factor an expression similar to the one proposed by Rhodes and Keck (Eq. 3), but in which the exponent is a linear function of the equivalence ratio.

$$f_2(x_d) = 1 - \mu_1 x_d^{\mu_2 + (\varphi - 1)\mu_3} \tag{5}$$

This expression was initially suggested by Clarke [17, 18] in a study on the propagation of fuel/air flames in zero gravity conditions. A few years later, Marshall *et al.* [19], in an extensive study on the laminar flame speeds of several neat liquid fuels (e.g., n-heptane, isooctane, toluene, ethylbenzene, and ethanol) diluted in real EGR obtained from preliminary explosions, employed a similar expression to quantify the dilution effect. The parametrization based on the experimental data showed that the values of the three parameters were strongly fuel dependent.

In their study on the laminar flame speeds of isooctane, n-butanol, and their blends, Fu *et al.* [20] expanded the original expression of Clarke by introducing a quadratic dependence of the exponent for the equivalence ratio to recover better the dependence of the dilution factor. Moreover, they offered a simple mixing rule able to calculate the dilution factor of a multicomponent EGR from the parameters of the neat diluents,

$$f_2(x_d) = 1 - \sum_{i=1}^{n} X_i \mu_{1,i} x_d^{\mu_{2,i} + \mu_{3,i}(\varphi - \varphi_{m,i}) + \mu_{4,i}(\varphi - \varphi_{m,i})^2} \tag{6}$$

where $\varphi_{m,i}$ is an arbitrarilly-set median equivalence ratio for the ith component in the EGR mixture. The authors also questioned the dependence of the dilution factor on the initial temperature and pressure, and concluded from kinetic modeling results that such dependence could be safely neglected.

Halter and co-workers [21–24] published a series of papers quantifying the effect of several diluents and additives on the propagation speed of isooctane/air flames. The diluent considered were N_2, CO_2, H_2O, and a ternary synthetic exhaust gas (N_2 / CO_2 / H_2O). The experimental observations indicate that diluent inhibition effectiveness decreases in the order: CO_2, H_2O, synthetic EGR, and N_2. The large collection of data was also used to propose an alternative to the traditional dilution factor expression by introducing the ratio,

$\nu_{O_2}/\nu_{O_2,ref}$, where ν_{O_2} is the ratio of oxygen in the non-fuel fraction of the mixture, i.e., $X_{O_2}/(X_{air} + X_{diluent})$, and $\nu_{O_2,ref}$ is the same ratio but for the reference mixture, which is the mixture without dilution. The dilution factor is then expressed as

$$f_4(\nu_{O_2}) = \left(\frac{\nu_{O_2}}{\nu_{O_2,ref}}\right)^{\gamma} \tag{7}$$

where the exponent γ is a linear function of the equivalence ratio [24]. The parametrization was only conducted for N_2 dilution, and γ was found to be weakly dependent on the equivalence ratio for isooctane ($d\gamma/d\varphi = 0.17$ and $\gamma \approx 2.65$).

More recently, Di Lorenzo *et al.* [25] measured the laminar flame speeds of a gasoline and its TRFE surrogate in air, either diluted (up to 20%) or not by synthetic EGR (13.62% CO_2, 12.22% H_2O and 74.16% N_2). Alongside the observation that the proposed TRFE surrogate was suitable to mimic the flame behavior of the real gasoline, even at diluted conditions, they successfully applied the dilution factor expression proposed by Galmiche *et al.* [23]. In contrast with the observations for N_2 diluted isooctane/air flames, a stronger dependence of the exponent γ to the equivalence ratio was reported for both the gasoline and its surrogate ($\gamma = 2.95 - 0.43\varphi$).

To sum up, several expressions for the dilution factor have been proposed (as listed in Table 1). These expressions got more complex as non-linear and equivalence ratio dependencies were introduced. Up to now, these modifications have always been proposed based on experimental observations and with the aim of retaining simple mathematical expressions.

Besides empirical correlations, Cho and Song [26] recently investigated the dilution effect on the ignition delay times from a theoretical perspective. They distinguished the non-chemical and chemical contributions. They related the former to the thermochemical properties of the diluent and the fuel/air mixtures, namely the ratio of constant volume heat capacities and the average Zeldovich number, whereas the latter is associated with the change in the overall mixture collision efficiency. They finally proposed a mathematical correlation suited for ignition delay times prediction. Although the conclusions of Cho and Song are only applicable to 0D-ignition, they could be the ground for a similar approach for flame propagation.

Table 1: Mathematical expressions from the literature modeling the dilution effect on the laminar flame speeds. x_d is the dilution ratio. Other parameters in the equations are described in the text.

No.	Equation	Fuel	Diluent	Max x_d	T (K)	P (bar)	φ	S_L database [a]	Ref.
1	$f(x_d) = 1 - ax_d$	isooctane, n-heptane, methanol, ethanol, methane, propane, IRMFD-303 (indolene)	N_2/CO_2 (85/15)	30%	300–700	0.4–50	0.7–1.4	Exp.	[9–12]
2	$f(x_d) = 1 - ax_d^b$	IRMFD-303 (indolene), RMFD-302	N_2/CO_2 (80/20)	30%	350–550	0.4–12	0.7–1.6	Exp.	[14]
3	$f(x_d) = (1 - ax_d)^b$	TRFE [b]	$CO_2/H_2O/N_2$	32%	300–600	4–8	1.0	Mod.	[15]
4	$f(x_d) = 1 - \mu_1 x_d^{\mu_2 + (\varphi - 1)\mu_3}$	commercial gasoline, n-heptane, isooctane, toluene, ethylbenzene, ethanol	N_2, real EGR	30%	310–450	0.5–4	0.7–1.3	Exp.	[16–19]
5	$f(x_d) = 1 - \sum_{i=1}^{n} X_i \mu_{1,i} x_d^{\mu}$ $\mu = \mu_{2,i} + \mu_{3,i}(\varphi - \varphi_{m,i}) + \mu_{4,i}(\varphi - \varphi_{m,i})^2$	isooctane, n-butanol	CO_2, H_2O, N_2, $CO_2/H_2O/N_2$	30%	428–500	1–5	0.7–1.5	Mod.	[20]
6	$f(\nu_{O_2}) = \left(\frac{\nu_{O_2}}{\nu_{O_2,ref}}\right)^{\gamma}$	isooctane, TRFE [b]	CO_2, H_2O, N_2, $CO_2/H_2O/N_2$	25%	373–473	1–10	0.8–1.5	Exp.	[21–25]

[a] Expt.= experimental data, Mod. = Kinetic Modeling.

[b] TRFE: Toluene Reference Fuel with Ethanol Addition, a gasoline surrogate composed of n-heptane, isooctane, toluene, and ethanol.

Nevertheless, some authors have already attempted to assess the non-chemical and chemical contribution of the dilution dumping effect on the laminar flame speed by using detailed chemical kinetic models. By considering fictitious species retaining only some properties of the diluent, the non-chemical and chemical contributions can be uncoupled. Such analyses demonstrated that the dilution effect of N_2 was almost exclusively dominated by its thermal properties, whereas thermal and chemical mechanisms were both important for CO_2 and H_2O. [21, 27, 28] The chemical mechanisms involved appear to be fuel independent, as they proceed through the interactions with the radical pool. Regarding CO_2, these interactions mainly consist in its reaction with the H atom ($CO_2 + H = CO + OH$) and its larger Chap-

eron efficiency promoting termination reactions such as $H + O_2 (+ M) = HO_2 (+ M)$ and $H + OH (+ M) = H_2O (+ M)$, and to a lesser extent with its reactions with CH_3, CH_2 and CH radicals. [28] For water, the chemical interactions remain less clear: besides its participation as an efficient third body collider in termination reactions, its participation in a large body of H-abstraction reactions may also displace some chemical equilibria. [29]

However, the aforementioned correlations show limitations as the interest is growing for combustion at more extreme conditions, such as over-lean and over-rich mixtures, high temperature, high pressure, and high dilution ratios. For example, the S_L vs. φ curve deviates from the quadratic shape as the equivalence ratio expands to over-lean and over-rich conditions. Indeed, it is asymmetric between the left (or "lean") and right (or "rich") branches: S_L decreases to an asymptotic value as φ approaches the flammability limits [30], unlike the faster decay predicted by the quadratic expression which would result in large uncertainties near the flammability limits. A similar limitation also holds for the temperature exponent [30], with only the convexity of the parabola being the opposite. Regarding the effect of dilution, an increasing number of studies suggest a non-linear dependence of S_L with the dilution ratio, but existing expressions show either inadequate fitting quality, large uncertainties, or unrealistic values at high dilution ratios. Deficiencies of these expressions originate from the lack or the limited set of experimental data at these unusual conditions. However, this situation can nowadays be fixed through kinetic modeling.

The aim of the present work is to propose new expressions for the laminar flame speed S_L correlation, especially for the reference S_L, temperature exponent, and dilution terms. These new formulations will then be applied to a Toluene Reference Fuel with Ethanol addition (TRFE) emulating a commercial gasoline fuel for which an experimental S_L database is available. This latter will then be extended through kinetic modeling, employing a kinetic mechanism specifically herein developed and validated for this surrogate. Finally, correlation parameters will be derived and the adequacy of the proposed empirical correlation will be discussed.

2. Empirical Correlation

As mentioned in the introduction, empirical correlations enabling quick estimation of the laminar flame speeds for a given set of conditions (T, P, equivalence ratio φ and dilution ratio x_d) are widely used in CFD modeling. In order to expand the validity of correlation to wider ranges of equivalence ratio, temperature, pressure, and dilution ratio, we propose a new correlation with novel expressions. The correlation formula takes the form expressed as Eq. 8, with addition of a correction term for dilution with respect to Eq. 1.

$$S_L(\varphi, T, P, x_d) = S_{L,ref}(\varphi)\left(\frac{T}{T_{ref}}\right)^{\alpha}\left(\frac{P}{P_{ref}}\right)^{\beta}\exp\left(-\frac{\mu x_d}{1-x_d}\right) \tag{8}$$

The details of each term in Eq. 8 are discussed in the following text of this section. It is noteworthy that the expressions discussed in this section are universal and apply to any fuel.

2.1. Reference Laminar Flame Speed

Since the pioneering work of Metghalchi *et al.* [31, 10], polynomial functions, especially second-order, have been preferentially used to fit laminar flame speeds. Indeed, both experimental measurements and modeling results show that the laminar flame speed dependence with the equivalence ratio exhibits a symmetry axis around $\varphi = 1.05$–1.10 for most of the fuels. Nevertheless, this observation does not hold for the very-lean and very-rich fuel branches, and the quadratic expression may then underestimate strongly the laminar flame speed, and even returns negative values. Some authors have circumvented this issue by adopting quartic expressions. [23] But, as shown thereafter, such expressions still underestimate the laminar flame speeds in very fuel-rich conditions while introducing new issues. Therefore, a different formalism is desired.

The behavior of the laminar flame speed on the fuel-lean and fuel-rich side is very different, and therefore each branch should be described by its own representative function. Moreover, the proposed expression should also be able to capture the first derivative of the laminar flame speed with respect to the equivalence ratio, especially the dampening usually observed in over-rich conditions [30], enabling a more realistic representation near the flammability limits. And ideally, the parameters involved in the expression would be related

to physical quantities. Within these considerations, we propose the following correlation in which Gaussian functions are preferred over polynomial expansions.

$$S_{L,ref}(\varphi) = \begin{cases} A_1 \exp\left[-\frac{1}{2}\left(\frac{\varphi-\varphi_m}{B_1}\right)^2\right] + (S_{L,max} - A_1), & \varphi > \varphi_m \\ A_2 \exp\left[-\frac{1}{2}\left(\frac{\varphi-\varphi_m}{B_2}\right)^2\right] + (S_{L,max} - A_2), & \varphi \leq \varphi_m \end{cases} \tag{9}$$

The new expression herein proposed requires six parameters, and they are associated with physical quantities as demonstrated in Figure 1a and 1b. $S_{L,max}$ is the maximum value of the laminar flame speed that is observed at the equivalence ratio φ_m. The parameter A_1 correspond to the difference between the $S_{L,max}$ and the laminar flame speed at the fuel-rich flammability limit. It is worth noting that although it should be the same for A_2 (in the fuel-lean branch) based on Eq. 9, fitting based on the limited data available would yield an A_2 value larger than $S_{L,max}$ and therefore negative S_L as φ approaches to zero. It indicates that a better and more realistic expression for the fuel-lean branch is still needed and subjects to further studies. The constants B_1 and B_2 are the equivalence ratio differences between the central value φ_m and the mixtures of maximum rates of S_L decrease and increase on the fuel-rich and fuel-lean branches, respectively, i.e., $\left(\frac{\mathrm{d}^2 S_L}{\mathrm{d}\,\varphi^2}\right)_{\varphi_m+B_1} = \left(\frac{\mathrm{d}^2 S_L}{\mathrm{d}\,\varphi^2}\right)_{\varphi_m-B_2} = 0$.

Figures 1a and 1b compare the fitting quality of the present correlation with the conventional quadratic expression as well as the quartic expression regarding the laminar flame speed and its derivative with respect to the equivalence ratio. A better agreement is observed on the whole equivalence ratio domain, especially at the edges. In contrast, the quartic expression exhibits an unrealistic nonmonotonic behavior at the over-rich edges, indicating its insufficiency for fitting laminar flame speeds at extreme equivalence ratios.

Moreover, the fitting capability of Eq. 9 is further validated based on the experimental flame speeds for $CH_4, C_2H_6,$ and C_3H_8 at over-rich conditions measured by Han *et al.* [30], as shown in Figure 2. For over-lean conditions, although the bending of the curve is usually less significant, the Gaussian function is also adpoted which could be helpful when new experimental data become available. These indicate that the use of Gaussian functions could better represent flame speeds for extreme (over-lean and over-rich) mixtures, and could help expand the validity of correlations in terms of equivalence ratio.

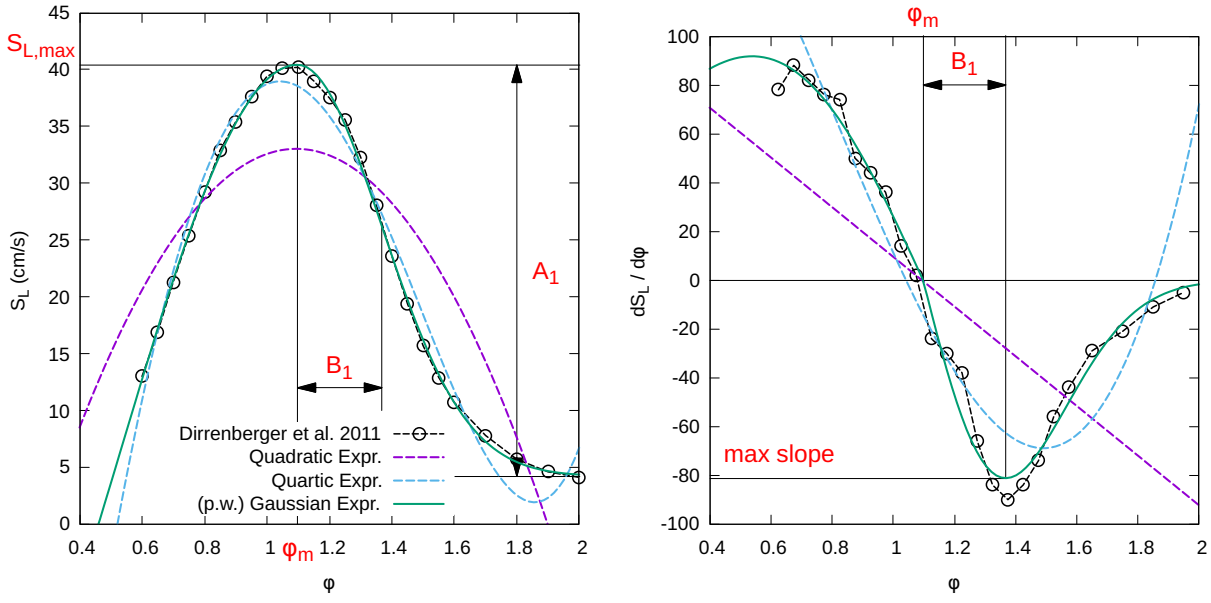

(a) S_L (b) $\mathrm{d}\,S_L/\mathrm{d}\,\varphi$

Figure 1: (a) Laminar flame speed and (b) its derivative $\mathrm{d}\,S_{L,ref}/\mathrm{d}\,\varphi$ as a function of equivalence ratio: comparison between the herein proposed Gaussian, the usual quadratic, and the more recent quartic expressions. The experimental data used as reference are propane/air flames at standard conditions (300 K, 1 atm) from Dirrenberger *et al.* [32].

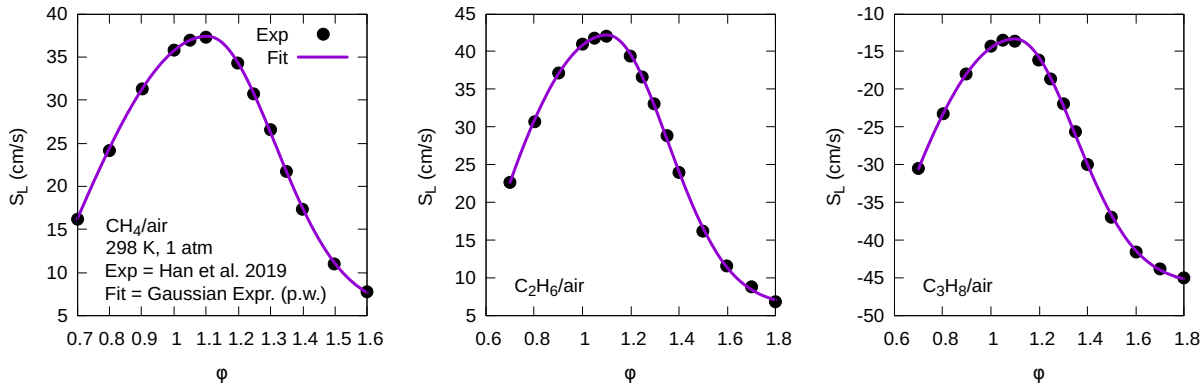

(a) CH_4/air (b) C_2H_6/air (c) C_3H_8/air

Figure 2: Laminar flame speed for (a) CH_4, (b) C_2H_6, and (c) C_3H_8: comparison between experimental data [30] and the herein proposed Gaussian expression.

2.2. Temperature Exponent

Similar to the reference flame speed correlation, quadratic formulas are widely used in the literature to model the temperature exponent. However, such functions result in a

temperature exponent that keeps increasing as the equivalence ratio increases or decreases, resulting in unrealistic large values away from the stoichiometry. Recent experimental data on C_1–C_3 alkanes [30], on the contrary, show that for fuel-rich mixtures the temperature exponent reaches an asymptotic value. Therefore, the step function consisting of two Gaussian functions, similar to the reference flame speed term, is also necessary to avoid problems of unrealistic (increasing) S_L at over-rich or over-lean conditions. With such considerations, we propose the following equation for the temperature exponent.

$$\alpha(\varphi) = \begin{cases} \alpha_0 + \alpha_{A_1} - \alpha_{A_1} \exp\left[-\frac{1}{2}\left(\frac{\varphi-\varphi_\alpha}{\alpha_{B_1}}\right)^2\right], & \varphi > \varphi_\alpha \\ \alpha_0 + \alpha_{A_2} - \alpha_{A_2} \exp\left[-\frac{1}{2}\left(\frac{\varphi-\varphi_\alpha}{\alpha_{B_2}}\right)^2\right], & \varphi \leq \varphi_\alpha \end{cases} \tag{10}$$

Similar to Eq. 9, α_0 is the maximum or minimum value of the temperature exponent which occurs at the equivalence ratio φ_α. α_{A_1}, α_{B_1}, α_{A_2}, α_{B_2} also have similar meanings on the curves as the A_1, B_1, A_2, and B_2 for $S_{L,ref}$, respectively.

Figure 3 shows the the comparison between the quadratic and Gaussian expression on fitting the laminar flame speeds and their temperature exponent. The reference data used for the fitting are for the TRFE fuel diluted by synthetic EGR, obtained by kinetic modeling using MACDIL Mech.. Thier information is available in Section 3. It can be seen from Figure 3a that the flame speeds generated using the conventional quadratic expression for the temperature exponent exhibit an unrealistic increase at fuel-rich conditions (φ=1.8–2.0). According to Figure 3b, this is due to the rapid increase of temperature exponent at rich conditions (from ≈ 3.4 at $\varphi = 1.8$ to ≈ 4 at $\varphi = 2.0$), which is much faster than predicted by MACDIL Mech.. In contrast with the quadratic expression, Eq. 10 results in a slower increase of $\alpha(\varphi)$ in the over fuel-rich region, and would eventually reach an asymptotic value.

In addition, the adequacy of Eq. 10 in modeling the temperature exponents is further demonstrated against the experimental data for n-heptane and isooctane flames reported by Han *et al.* [33] as displayed in the *Supplementary Material*.

It is noteworthy that although Eq. 10 is an improvement over the traditional quadratic expression, it cannot eliminate completely the temperature exponent overestimation issue at $\varphi > 2$, especially if neither experimental nor modeling data are available to constraint

the parameters optimization.

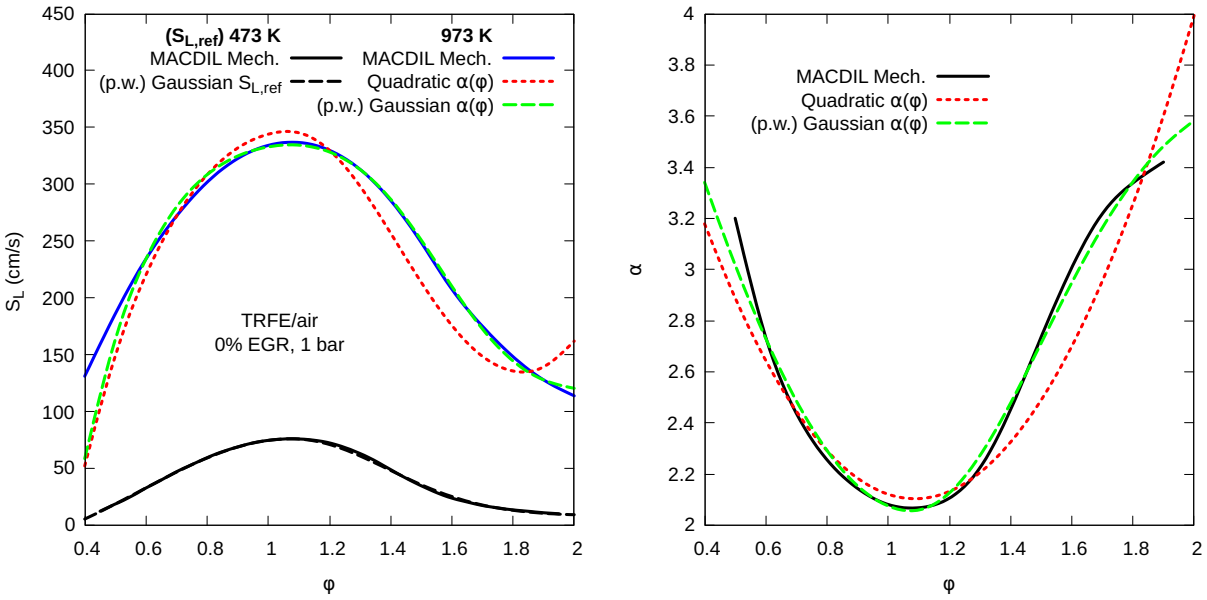

(a) S_L (b) α

Figure 3: Comparison between (a) the laminar flame speeds (473 K and 973 K, 1 bar) and (b) the equivalence ratio dependent temperature exponent $\alpha(\varphi)$ with either a quadratic or a Gaussian expression (Eq. 10) for the temperature exponent. The reference data used are for the TRFE fuel diluted by synthetic EGR, computed using MACDIL Mech.. (See Section 3)

2.3. Pressure Exponent

Since the early developments of the asymptotic theory of premixed flame, laminar flame speed is known to decrease with the pressure ($S_L \propto \mathrm{P}^{\beta}$) with exponent β in the $[-1, 0)$ interval. Such behavior has been experimentally confirmed, regardless of the fuel or the equivalence ratio. Because of the complex chemistry involved in combustion, this exponent changes with the mixture composition and therefore equivalence ratio dependent expressions are required in the laminar flame speed correlations. Most of the recent studies adopted a quadratic polynomial for β, and the present correlation stick with this usage,

$$\beta(\varphi) = \beta_0 + \beta_2(\varphi - \varphi_\beta)^2 \tag{11}$$

where φ_β is the equivalence ratio where the quadratic β-φ curve is at its symmetrical axis.

2.4. Dilution Factor

Another originality of the present correlation is the formulation for the dilution factor $f(x_d)$. We propose an exponential expression

$$f(x_d) = \exp(-\frac{\mu x_d}{1 - x_d}) \tag{12}$$

which has the following mathematical characteristics to better match the evolution of S_L with the dilution ratio x_d: (i) $f(0) = 1$, i.e., the function is equal to unity at non-diluted case ($x_d = 0$); (ii) $\lim_{x_d \to 1} f(x_d) = 0$, i.e., the function approaches asymptotically to zero as the dilution ratio keeps increasing; (iii) $f'(x_d) < 0, \quad 0 \leq x_d < 1$, i.e., the function decreases monotonically; (iv) $\lim_{x_d \to 1} f'(x_d) = 0$, i.e., the reduction effectiveness decreases as the dilution ratio gets higher.

Because of the above characteristics, the proposed dilution term outperforms other existing formulas in the literature in capturing the dilution effect. Figure 4a compares calculated laminar flame speeds for EGR dilution ratio up to 50% (higher dilution ratio could not be reached because of numerical unstabilities due to the very low flame speeds) with the different dilution terms discussed above. As it can be seen in this figure, expressions $f_1(x_d)$ (Eq. 2) and $f_2(x_d)$ (Eq. 3) generate unrealistic negative values at high dilution. The expression $f_4(x_d)$ (Eq. 7) proposed in Ref. [25] could fit well at low dilution but deviates from data at higher dilution, e.g., $x_d > 0.4$. Although expression $f_3(x_d)$ (Eq. 4) fits well the data, it reaches zero at $x_d = 1/a$ and yield erroneous values at $x_d > 1/a$ (either negative or positive depend on the value of parameter b). Only Eq. 12 ($f_0(x_d)$ in the figure) could fit well the data and prevent yielding unrealistic values at all conditions at the same time.

In addition, the only parameter introduced in this expression, μ, relates to a physical property: it is the S_L reduction effectiveness of the diluent (or the diluent mixture) at zero-dilution, $\mu = -f'(0)$. The higher the parameter μ is, the stronger (more effective) the diluent is in reducing flame speeds, as shown in Figure 4b. For example, CO_2 is more efficient in reducing S_L than H_2O, so the parameter μ for CO_2 is higher than that of H_2O. Therefore, the formula proposed in the present work has the advantage of good fitting performance while preventing unrealistic output values, and using only one parameter which could indicate the

dilution effectiveness of the diluent.

As it will be illustrated later, the dilution effect, i.e. the dilution effectiveness, is found to vary with the equivalence ratio according to a quadratic polynomial: the dilution effectiveness is minimum near the stoichiometry and increases as the equivalence ratio shifts towards the fuel-lean and fuel-rich sides. Moreover, the dilution effectiveness may also depend on the initial temperature and pressure, and it must be accounted for in the final expression of μ. Therefore, the combination of a quadratic φ-dependence with two power terms for the T- and P-dependences is proposed,

$$\mu = \left(\mu_0 + \mu_2(\varphi - \varphi_\mu)^2\right) \left(\frac{T}{T_{ref}}\right)^{\mu_\alpha} \left(\frac{P}{P_{ref}}\right)^{\mu_\beta} \tag{13}$$

where φ_μ is the equivalence ratio where the symmetrical axis of the φ-dependence is located, and μ_α and μ_β are the power exponents for the T- and P-dependences, respectively.

Furthermore, for mixture diluents such as EGR, we suggest to estimate the dilution effectiveness of the mixture μ_{mix} based on the dilution effectiveness of each EGR components using a linear mixing rule,

$$\mu_{mix} = \sum_i X_i \mu_i \tag{14}$$

where X_i and μ_i are the mole fractions and dilution effectiveness of the components. The validity is assessed indirectly based experimental values and discussed later in the paper.

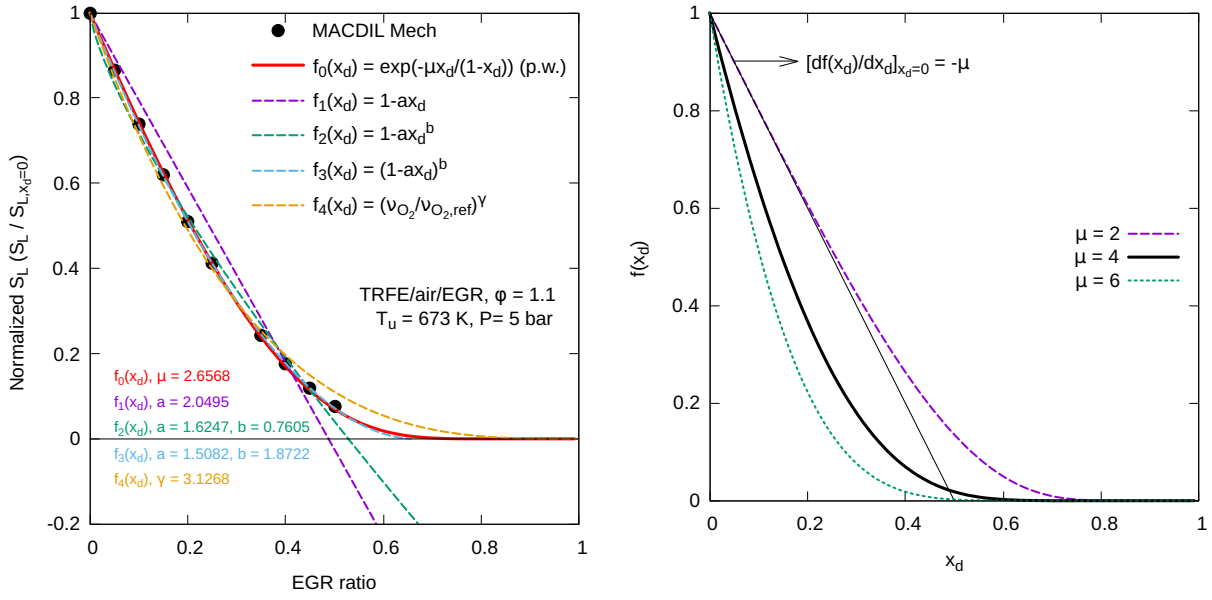

(a) Comparison on fitting performance

(b) Effect of μ

Figure 4: (a) Comparison between the training computed laminar flame speed data set (MACDIL Mech. computations) and the predictions based on the different dilution term expressions discussed in the main text and (b) effect of changing the dilution effectiveness μ on the herein proposed dilution term $f(x_d)$ (Eq. 12). The reference data used are for the TRFE fuel diluted by synthetic EGR, computed using MACDIL Mech.. (See Section 3)

3. Fuel selection and kinetic modeling

Empirical correlations, regardless of their mathematical accuracies, are heavily dependent on the data used as the training set. Experimental data are scarce and usually limited to narrow pressure, temperature, and dilution ratio ranges, but validated kinetic models can help extend these databases. In this section, after introducing the fuel selected for the present case study, a related kinetic model is assembled and tested against the experimental data available.

3.1. Choice of Fuel and Available Data

The EGR technology for next-generation engines will be optimized for gasoline fuels, as many countries in Europe have already enacted the ban of diesel engines and fuel by the 2030s. The present study is part of a larger multi-team effort, MACDIL, aiming at better characterizing the oxidation and the flame propagation of a particular gasoline fuel under diluted conditions. This fuel is the commercial gasoline B71 1188 ESSH EURO5 + 20. It contains 5% ethanol and has a RON and a MON of 96 and 88, respectively. Other properties of this fuel, reported originally by Di Lorenzo *et al.* [25], are given in Table 2.

Di Lorenzo *et al.* [25], as members of the project MACDIL, have experimentally demonstrated that the commercial gasoline of interest could be emulated by a Toluene Reference Fuel with Ethanol addition (TRFE) composed of 44% isooctane, 15% n-heptane, 36% toluene, and 5% ethanol in liquid volume fractions, labeled TAE 7500 gasoline. Table 2 compares the properties of the surrogate and the commercial fuels. Thereafter, we will refer to this specific surrogate using the abbreviation "TRFE".

Di Lorenzo *et al.* [25] measured the laminar flame speeds of TRFE in air (N_2 / O_2 = 79%/21% by volume), without and with the dilution of synthetic EGR in a spherical combustion vessel equipped with a double-view Schlieren configuration, enabling to constantly assess the anisotropy of the propagating flame. The synthetic EGR composition was set to 74.16% N_2, 13.62% CO_2, and 12.22% H_2O on a molar basis. The authors defined the EGR ratio as $X_{\mathrm{EGR}}/(X_{\mathrm{fuel}} + X_{\mathrm{air}} + X_{\mathrm{EGR}})$, and this definition has been adopted hereafter. Data were collected over a large set of conditions: equivalence ratios ranging from 0.85 to 1.40,

Table 2: Comparison on the properties and composition of one commercial gasoline and the TRFE surrogate. Reproduced from Ref. [25].

Gasoline *(B71 1188 ESSH EUROS + 20)*		TRFE surrogate *(for TAE 7500 gasoline)*	
properties:			
RON	96.6	RON	95
C/H/O (mass%)	85.1/13.1/1.8	C/H/O (mass%)	84.79/13.34/1.87
ρ (kg/m^3) (at 15 °C)	753.0	ρ (kg/m^3) (at 15 °C)	750.5
composition (liq.vol.%):			
ethanol	5.0	ethanol	5.0
n-heptane	3.6	n-heptane	15.0
isooctane	50.0	isooctane	44.0
aromatics	33.7	toluene	36.0
(benzene)	(0.1)		
olefin	6.2		
methyl-cyclohexane	1.5		

temperatures of 373, 423, and 473 K, pressures between 1 and 5 atm, and EGR ratios of 0, 10, and 20%. Though comprehensive, experimental apparatus limitations prevented reaching higher temperatures and pressures that can be encountered in the engine combustion chamber. Further details on the experimental measurements and the exact content of the database can be found in [25].

3.2. Development of the Reduced Model

The surrogate fuel selected for this study is a mixture of n-heptane, isooctane, toluene, and ethanol. Kinetic models for gasoline fuels encompassing these four components have already been published. Especially, Mehl *et al.* [34] released such a kinetic model, referred hereafter as LNLL2011, validated on speciation data obtained in flow reactors and ignition delay times. However, this mechanism had not been initially developped for gasoline surrogates with ethanol and tested against laminar flame speeds. Over the last decade,

no updates have been proposed for this mechanism, especially for the pressure-dependent and third-body reactions that may be sensitive in higly-diluted conditions. In addition, advances have been seen since then on detailed kinetic mechanisms for the aforementioned fuel components as well as core C_0-C_4 mechanisms for hydrocarbon combustion. Therefore, rather than modifying and updating an existing model, the decision was made to assemble a new kinetic model that would include both the low-temperature and high-temperature chemistries of the four molecules in TRFE.

Aramco Mech 3.0 [35], a comprehensive mechanism for the oxidation of C_0–C_4 hydrocarbons, has been adopted as the core sub-mechanism. However, the ethanol subset has been substituted by the one published by Zhang *et al.* [36]. The sub-mechanisms of n-heptane (and related species) from Zhang *et al.* [37], of isooctane from Atef *et al.* [38], and of toluene from Yuan *et al.* [39, 40] were then added to the core reaction set. Care was taken during the merging of the different subsets to remove duplicate species and reactions, and to homogenize the species nomenclature. Identified missing reactions were adopted from the LLNL 2011 mechanism. Thermochemical and transport data for each species were inherited from their parent mechanisms. The list of sub-mechanisms used in the inital construction of the detail mechanism and their relative priorities is shown in Table 3.

Table 3: List of sub-mechanisms and their priorities during the construction of the detail mechanism.

Priority[a]	Sub-mechanism	Main Fuel	Ref.
1	LLNL2011	Gasoline Surrogate	[34]
2	Zhang *et al.* 2016	n-heptane	[37]
3	Atef *et al.* 2017	Isooctane	[38]
4	Yuan *et al.* 2015	Toluene	[39, 40]
5	Aramco Mech. 3.0	C_0-C_4	[35]
6	Zhang *et al.* 2018	Ethanol	[36]

[a]The parameters for duplicated species and reactions are replaced by the parameters from the sub-mechanism with the highest value in priority.

Despite that Aramco Mech 3.0 is a recent model, rate coefficients of some reactions potentially sensitive for laminar flame speeds predictions have been the focus of even more recent publications. Hence, the original rate constants for these reactions were updated. They mainly consist in reactions of the C_2–C_3 sub-mechanism. For example, Xiong *et al.* [41] and Mai *et al.* [42] investigated theoretically the reaction of ketenyl radicals with hydroxyl radicals (HCCO + OH). They both found that the reaction can proceed either on a singlet or triplet potential energy surface, and concluded that HCOH (either singlet or triplet) is the main reaction outcome. Singlet HCOH then further dissociates into H_2 + CO or undergoes an isomerization into formaldehyde (CH_2O). Xiong *et al.* derived high-pressure-limiting rate constants for the different paths identified, and they were included in the present model. Likewise, the reactions of ketene with free radicals, such as OH, CH_2, and CH_3, are receiving growing interest because of their potential significance to flame speeds [43, 44] and have thus been the subject of several recent articles [45–47], the conclusions of which have been included in the detailed model. Further rate constants have been updated and the reader is invited to refer to the detailed description presented in Section S3 of the *Supplementary Material*. The model is also provided in the *Supplementary Material* for further details.

At this stage, the kinetic model consists of 2339 species involved in 9440 reactions, which is prohibitive to perform flame speed calculations. In order to lower the cost of one-dimensional calculations while maintaining the model accuracy, a reduction procedure based on adiabatic constant-volume 0-D homogeneous reactor is applied. By selecting a high initial temperature and target properties relevant to flame speeds (heat release and concentration of small radicals), this strategy (i) removes low temperature (ii) while retaining high-temperature chemistry important for laminar flame speed calcualtions (iii) over a large range of temperature and pressures encountered at later times in the reactor. The Direct Relation Graph method with Error Propagation (DRGEP) followed by a full sensitivity analysis is applied for the reduction procedure, as implemented in Chemkin Pro software [48]. TRFE/air/EGR mixtures are considered for the reactants and the matrix of initial conditions is as follows: φ = 0.8-1.1-1.4, T_i = 1000 K, P_i = 1-5 bar and EGR ratio =

0-20-50%. This matrix, applied to zero-dimensional constant volume calculations, covers a wide range of temperature (1000–3000 K) and pressure (1-17 bar) to emulate the conditions encountered throughout the reaction zone of 1-D flames, where the high-temperature combustion chemistry relevant to flame conditions is favored. Target properties were ignition delay time (IDT), maximum heat release rate, maximum integrated heat release, maximum mole fractions for H, OH, HO_2, and CH_3 radicals, with a maximum error tolerance of 5%. A list of the parameters used during the DRGEP reduction process is presented in the *Supplementary Material*, as well as a comparison between the ignition delay times computed by the detailed and reduced mechansims. It shows that the reduction strategy succeeded in retaining only the high temperature chemistry relevant to flames. This final reduced mechnism encompasses 593 species and 3698 reactions, and is referred to as the MACDIL Mech. thereafter.

3.3. Validation of the Reduced Model

Before using MACDIL Mech. to extend the database published by Di Lorenzo *et al.* for the TRFE surrogate fuel, it is tested and validated against experimental laminar flame speeds measurements available in the literature for TRF and TRFE fuels.

The PREMIX code [49] included in the CHEMKIN Pro software [48] was employed to perform the laminar flame speed calculations. A 20 cm wide domain and fine grid control parameters (GRAD=0.1 and CURV=0.1) were used to ensure freely propagating flames as well as grid-independent results. Thermal diffusion (Soret effect) was included. Mixture average transport was used instead of multi-component transport to reduce computational time. Comparisons have been performed (included in the *Supplementary Material*) and showed that the simplified mixture-average calculations are in very close agreement with the multi-component flame speeds, with absolute differences ranging from 0.01 to 0.57 cm/s and relative differences ranging from 0.16% to 2.67%.

3.3.1. Validation on Pure Component and TRF Mixtures

In a first attempt to validate the model, the ability of MACDIL Mech. to predict the laminar flame speeds of the four components has been assessed. These comparisons are

provided in the *Supplementary Material*. The model exhibits an overall good agreement for the four fuels, although laminar flame speeds predicted for isooctane and ethanol are close to the lower bound of the experimental uncertainties.

Figure 5a displays the comparison between the present predictions and the experimental data of Mannaa *et al.* [50] obtained for a TRF surrogate at different initial pressures and in a wide equivalence ratio range (0.8–1.6). The experimental data were obtained by monitoring the outward propagation of spherical flames in a heated combustion vessel. The TRF surrogate used for the experiments has a composition (on a liquid volume basis) of 77.4% isooctane, 17.6% n-heptane, and 5% toluene. For equivalence ratios between 0.8 and 1.3, MACDIL Mech. predictions agree well with the experimental value, with deviations less than 2 cm/s. At very fuel-rich conditions, predicted flame speeds are significantly lower than the experimental observations, up to 5 cm/s at $\varphi = 1.6$. Such deviations suggest that the MACDIL mechanism can be further improved, although these disparities may also be attributed to some extent to experimental uncertainties, especially on the equivalence ratio.

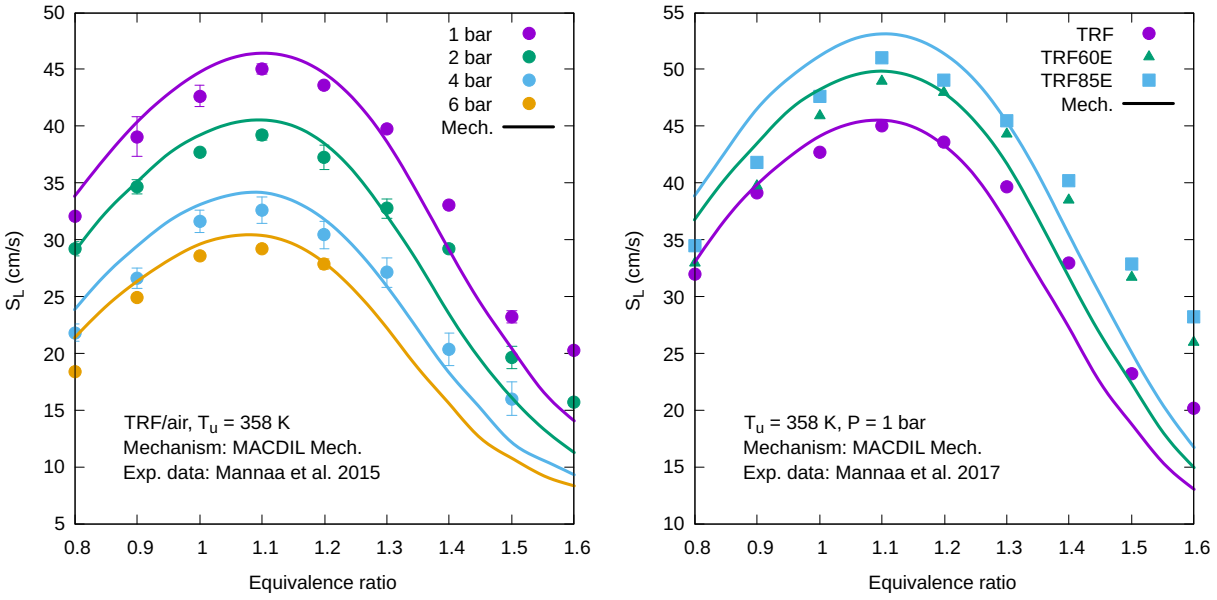

(a) TRF

(b) TRF/ethanol mixture

Figure 5: Laminar flame speeds for a TRF surrogate. (a) Effect of pressure [50], and (b) effect of ethanol addition [51]. Experimental data are displayed as symbols and MACDIL Mech. calculations as solid lines.

Mannaa *et al.* [51] also investigated the effect of blending ethanol to the TRF, and they observed that the laminar flame speed increases with the ethanol amount, regardless of the equivalence ratio. A similar trend is predicted by MACDIL Mech., as it can be seen in Figure 5b. Moreover, the agreement between the experimental values and the predicted ones around the stoichiometry is consistent with the observations without ethanol addition (deviations less than 5 cm/s) whereas large discrepancies (up to 10 cm/s) exist for very fuel-rich mixtures with high amounts of ethanol. In their study, Mannaa et al. [51] performed kinetic modeling using the LLNL2011 mechanism and observed similar deviations at the fuel-rich conditions.

3.3.2. Validation on the Targeted TRFE Surrogate

The fundamental laminar flame speeds of the target TRFE surrogate have been measured by Di Lorenzo *et al.* [25] in a spherical vessel, and the influence of four parameters on S_L has been evaluated: equivalence ratio, temperature, pressure, and EGR ratio.

Effect of Temperature and Equivalence Ratio

The predictions of MACDIL Mech. are compared to the experimental values at atmospheric pressure and three different inlet temperatures (373, 423, 473 K) without EGR in Figures 6a–6c. For reference, the predictions of the LLNL 2011 [34] model are also displayed. For the three temperatures considered, the flame speeds computed with MACDIL Mech. are close to the measured values, within 5 cm/s (or 10% on a relative basis), for equivalence ratios up to 1.2. Beyond $\varphi = 1.2$, the predicted S_L are systematically lower than the experimental ones. The measurements do not exhibit a clear maximum flame speed since Di Lorenzo *et al.* [25] reported almost similar laminar flame speeds for equivalence ratio between 1 and 1.2 at the three temperatures. On the contrary, the present mechanism computes the maximum flame speed for equivalence ratio around $\varphi = 1.1$, which is in line with experimental observations for the pure components. Although both models are in qualitative agreement, the LLNL 2011 computed flame speeds are 2 to 5 cm/s larger than MACDIL Mech. predictions, and therefore significantly higher than the experimental values for equivalence ratios below 1.2.

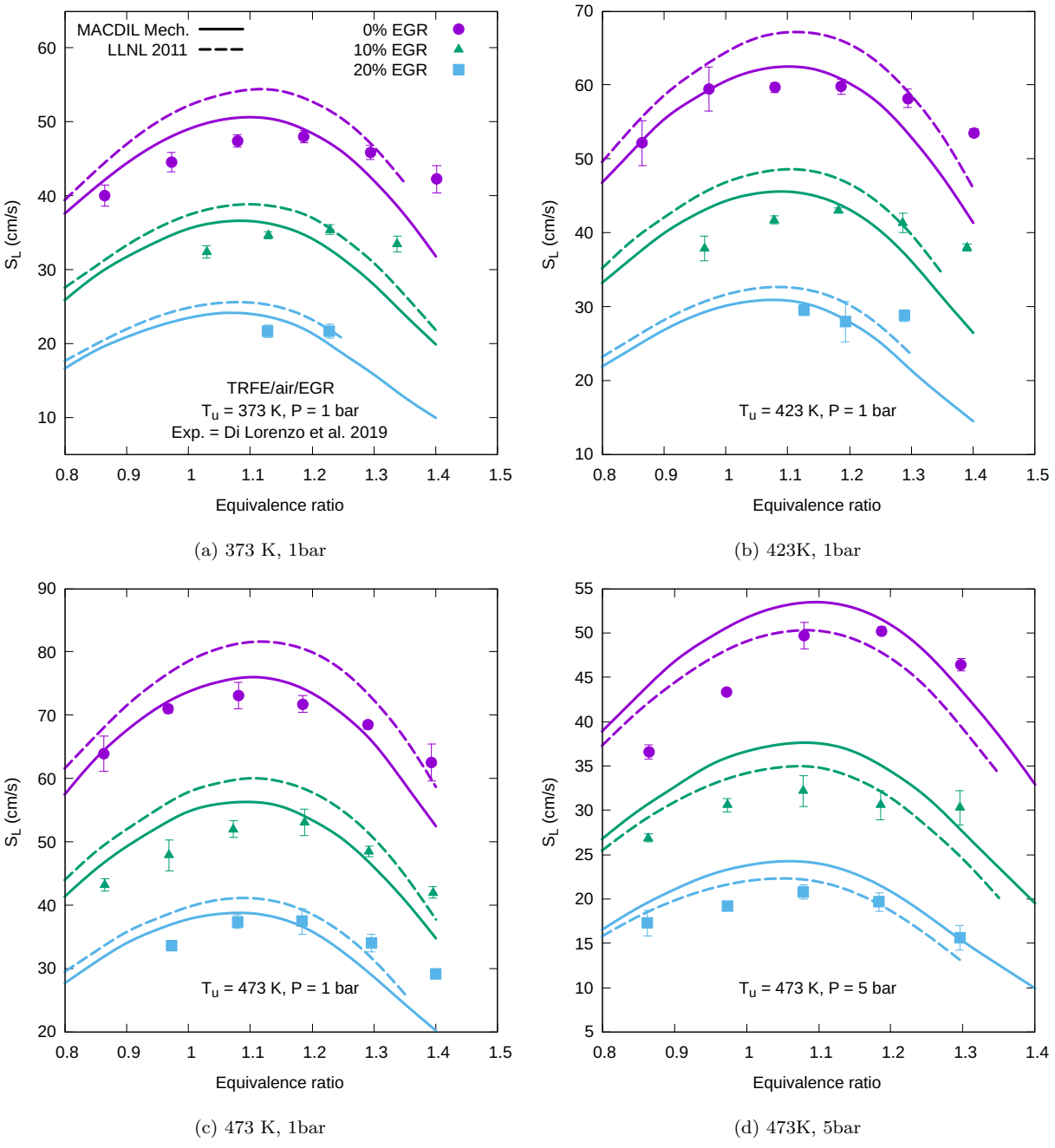

(a) 373 K, 1bar

(b) 423K, 1bar

(c) 473 K, 1bar

(d) 473K, 5bar

Figure 6: Laminar flame speed of TRFE/air/EGR mixtures: (a) 373 K and 1 bar; (b) 423 K and 1 bar; (c) 473 K and 1 bar; (d) 473 K and 5 bar. Experimental data [25] are displayed as symbols, the MACDIL Mech. and the LLNL model [34] calculations are displayed as solid and dashed lines, respectively.

Figure 7 depicts the temperature dependence of the laminar flame speed at an equivalence ratio of around 1.1. As expected, the laminar flame speeds increase with the temperature,

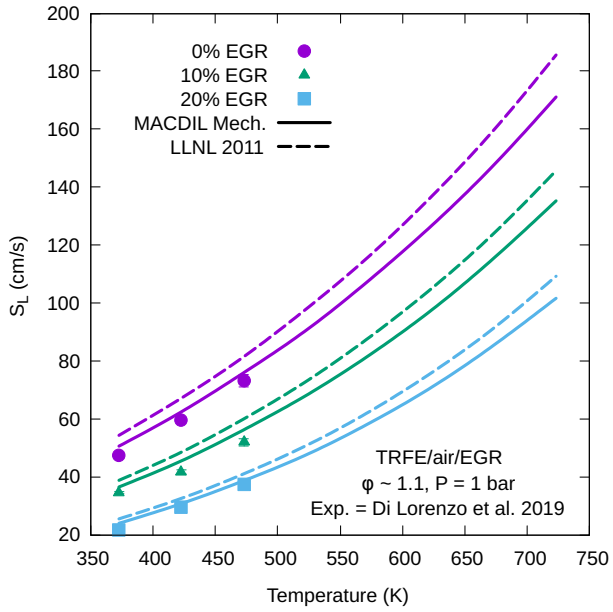

Figure 7: Effect of temperature on the laminar flame speed of TRFE/air and TRFE/air/EGR mixtures at 1 bar and $\varphi \approx 1.1$. Experimental data [25] are displayed as symbols, the MACDIL Mech. and the LLNL model [34] calculations are displayed as solid and dashed lines, respectively.

which is well captured both qualitatively and quantitatively by the two models. As already observed in Figures 6a–6c, the MACDIL Mech. predictions are nevertheless in better agreement with the experimental values. While the limited set of data suggests a linear dependence on the temperature, the modeling data unambiguously show that an exponential dependence is most likely. Using the apparent linear dependence would lead to a laminar flame speed of 130 cm/s for the TRFE/air mixture, whereas the model prediction is close to 160 cm/s, resulting in a deviation of nearly 20%.

Effect of Pressure

Di Lorenzo *et al.* investigated the effect of an increase of the pressure on the fundamental laminar flame speed of the TRFE surrogate. The pressure was varied between 1 and 5 bar. Figure 6d compares the experimental measurements at 473 K with the model predictions at the upper pressure. Unlike the observation at atmospheric pressure, MACDIL Mech. overestimates the laminar flame speeds on the fuel-lean side whereas a much better agreement

is obtained for $\varphi = 1.2$ and 1.3. The maximum flame speed is still predicted by the model to occur around $\varphi = 1.1$, but experimental data rather suggest an optimum at a slightly higher equivalence ratio. The LLNL 2011 model qualitatively agrees with the MACDIL Mech. computations, but its predicted laminar flame speeds are slower than the MACDIL ones even though the opposite trend was observed at atmospheric pressure. This observation suggests that the pressure dependence of the laminar flame speed is more pronounced in this model. Figure 8 displays the dependence of S_L to the pressure according to the two models and the experimental measurements for near stoichiometric mixtures ($\varphi \approx 1.1$). Both experimental and numerical data exhibit a non-linear decay with the pressure, which is in line with the asymptotic theory that predicts S_L to be proportional to P^{β}, with β between -1 and -0.5. The experimental trend is well captured by MACDIL Mech., but the LLNL 2011 over-predicts the pressure dependence. Hence, while the LLNL 2011 computed laminar flame speeds are higher than that by MACDIL Mech., an inversion is detected for pressure around 2.5 atm and they are lower above this threshold.

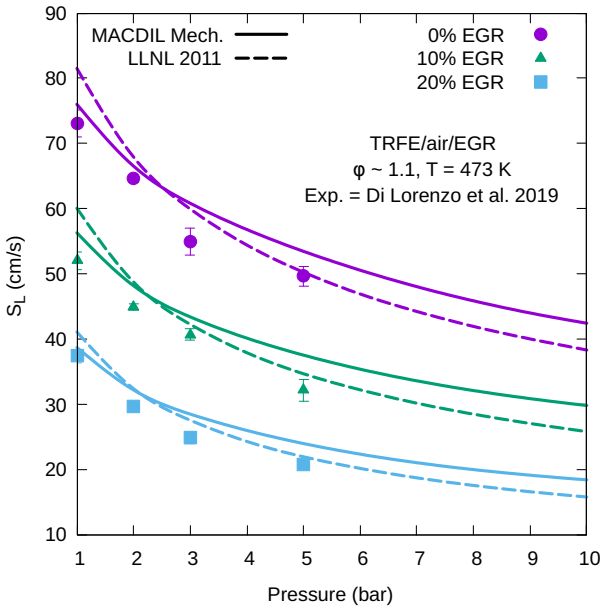

Figure 8: Effect of pressure on the laminar flame speed of TRFE/air/EGR mixtures at 473 K and $\varphi \approx 1.1$. Experimental data [25] are displayed as symbols, the MACDIL Mech. and the LLNL model [34] calculations are displayed as solid and dashed lines, respectively.

Effect of EGR Addition

Finally, the ability of MACDIL Mech. to account for the dilution effect on the laminar flame speed is tested. Di Lorenzo *et al.* [25] measured the laminar flame speeds of TRFE/air mixtures diluted by 10 and 20% of EGR. The experimental data are compared to the two mechanisms predictions in Figures 6a–6c. The observations previously made in the undiluted cases still hold with EGR addition: a maximum flame speed predicted around $\varphi = 1.1$ whereas experimental values rather suggest $\varphi = 1.2$, computed laminar flame speeds are higher than the experimental data on the fuel-lean side but lower for fuel-rich mixtures, and the LLNL 2011 predictions are higher than the MACDIL ones. However, the discrepancies between the two mechanisms shrink with the increase of the EGR dilution ratio, from ~ 5 cm/s at 0% to ~ 1.5 cm/s at 20% for $\varphi = 1.1$. This apparent reconciliation between the two models is actually a scaling effect, since as the dilution ratio increases, the laminar flame speed, and so the absolute difference between the two models, decreases but the relative difference remains constant, around 6% at $\varphi = 1.1$ regardless of the EGR ratio or initial temperature.

Figures 7 and 8 compare the experimental and computed temperature and pressure dependences of the laminar flame speeds for different EGR dilution ratio at near stoichiometric conditions. The agreement between the experimental and the computed S_L improves as the EGR ratio increases, although MACDIL Mech. slightly overestimates the laminar burning velocity. Nevertheless, the model computes an overall pressure and temperature dependence that are weakly, if none, sensitive to the EGR dilution ratio, which is consistent with the experimental observations despite the narrow experimental temperature and pressure ranges.

The effect of the EGR dilution ratio at constant temperature and pressure on the laminar flame speed of TRFE is displayed in Figure 9a. Over the range (0-20%) investigated by Di Lorenzo *et al.*, both a qualitative and quantitative agreement is observed between the experimental data and the computations using MACDIL Mech. and LLNL 2011. However, although the measurements might suggest a linear dependence of the laminar flame with

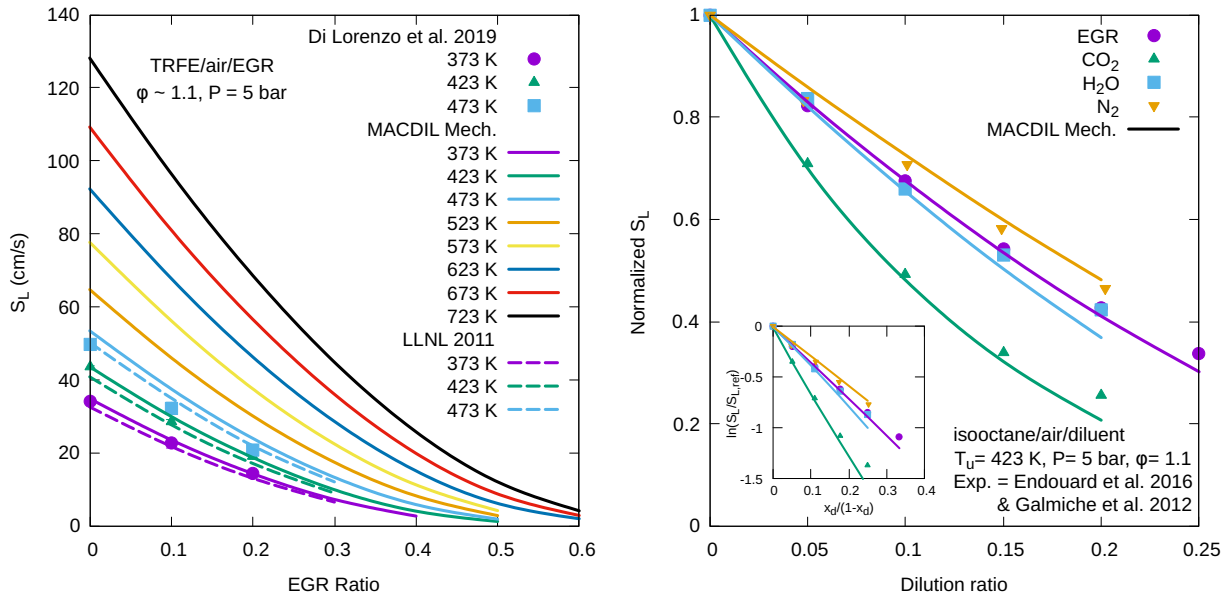

(a) TRFE

(b) isooctane

Figure 9: (a) Effect of the dilution ratio x_d on the laminar flame speeds of TRFE/air/EGR mixtures (phi=1.1, 5bar ; see main text for EGR composition) at different temperatures (symbols are experimental data [25], solid and dashed lines are MACDIL Mech. and LLNL model [34] calculations, respectively). (b) Effect of the diluent composition on the normalized laminar flame speeds of isooctane/air/diluent mixtures (phi=1.1, 423 K, 5 bar [24] [23]) ; normalized S_L is the ratio of the flame speed over the S_L at a referece condition, i.e., $S_L/S_{L,ref}$, which in this case is the flame speed at the non-diluted condition; the insert of Fig (b) displays the linearity between $\ln\left(\frac{S_L}{S_{L,ref}}\right)$ and $\frac{x_d}{1-x_d}$, with the slope being equal to the reduction effectiveness μ of the diluent.

the dilution ratio, this observation must be mitigated by the limited set of data and the uncertainties associated. The MACDIL mechanism on the contrary predicts a non-linear relationship between the two quantities (S_L and EGR ratio). In spite of the lack of experimental data at temperatures above 473 K, calculations with MACDIL Mech. are nonetheless displayed in Figure 9a as they show that the dilution effect is temperature dependent, with a stronger dependence at high temepratures. Indeed, one can clearly see that as the dilution ratio increases, the effectiveness of the diluent in reducing the laminar flame speeds decreases: dS_L/dx_d = -300, -220, and -120 cm/s for x_d = 0.1, 0.3, and 0.5, respectively at 723 K.

The EGR employed by Di Lorenzo *et al.* is a ternary mixture (CO_2 / H_2O / N_2), and therefore the overall effect observed is a combination of the thermal and chemical effects of the three components. Although no data are available for the targeted surrogate fuel diluted in each of the EGR components, Galmiche *et al.* [23] and Endouard *et al.* [24] carried out such measurements for isooctane/air mixtures, considering dilution in N_2, CO_2, and H_2. Since the surrogate fuel comprises nearly 50% of isooctane, the measurements of Endouard *et al.* can be used to assess the ability of MACDIL Mech. to capture the dilution effectiveness of these two diluents. This comparison is displayed in Figure 9b, in which the normalized flame speeds (with respect to the non-diluted case) of near stoichiometric isooctane/air mixtures are reported as a function of the dilution ratio. It can be seen that MACDIL Mech. exhibits good overall agreement with measurements. Consistent with the experimental observations, CO_2 is computed to be the most effective diluent in slowing down the flame propagation. While the mitigating effect of N_2 and H_2O on S_L is similar yet less than the one of CO_2 according to the experimental measurements, MACDIL Mech. computes slightly lower flame speeds for H_2O and slightly higher ones for N_2, yielding larger difference in dilution effect.

From the results in Figure 9b, the dilution effectiveness μ of these three molecules can be derived by plotting $\ln(S_L/S_{L,ref})$ as a function of $x_d/(1-x_d)$ according to the dilution efficiency expression proposed in this study (Eq. 12). The insert in figure 9b shows that a linear relationship is indeed obtained, leading to the following effectiveness (in descending order) for the three pure diluents: $\mu_{CO_2} = 6.06$ (6.45), $\mu_{H_2O} = 3.56$ (3.95), and $\mu_{N_2} = 3.10$ (2.91) (The values in brackets are those derived from the modeling results). With the same approach, the dilution effectiveness of the ternary mixture, the synthetic EGR, is close to the one of H_2O: $\mu_{EGR} = 3.41$ (3.56). These data are summarized in Table 4 along with the composition of the EGR mixture.

The knowledge of the dilution effectiveness of the three pure diluents and the mixture enable assessing the validity of the linear mixing rule proposed earlier (14), at least for this mixture and fuel. According to the mixture rule, the dilution effectiveness of the EGR mixture is calculated to be 3.56 from the experimental values of the three components, which

Table 4: Dilution effectiveness μ (Eq. 14) of several diluents and their mixtures derived from experimental measurents and mechanism predictions (Figure 9b)

.

Component	Mole Fraction	μ_i	μ_{EGR}	μ_{EGR} estimated by Eq. 14
Experimental Measurements				
N_2	74.16%	3.10		
H_2O	12.22%	3.56	3.41	3.56
CO_2	13.62%	6.06		
MACDIL Mech.				
N_2	74.16%	2.91		
H_2O	12.22%	3.95	3.56	3.52
CO_2	13.62%	6.45		

is very close to 3.41 according to the experimental measurements. Using the data based on the model predictions, an estimation of 3.52 is derived, which is even closer to the value, 3.56, obtained with the mechanism. Therefore, it may be possible to quickly calculate the dilution effectiveness of an arbitrary diluent mixture, providing the dilution effectiveness of neat diluents, which could greatly simplify the estimation of S_L for complex mixtures and extend the validity range of the empirical correlation. However, further investigations are still necessary to provide comprehensive proof or validation of this assumption, i.e., linear mixing rule of dilution effectiveness.

4. Correlation parameters for TRFE and its Predictive Perfomance in S_L

4.1. Generation of the database and determination of the correlation parameters

The reduced kinetic mechanism MACDIL Mech. described in the previous section has been used to extend the experimental database of Di Lorenzo*et al.* [25]. The final database for the laminar flame speeds of TRFE/air/EGR mixtures covers fresh gas temperatures between 373 and 973 K, pressures from 1 to 50 bar, equivalence ratios from 0.4 to 2.0, and EGR dilution ratios between 0 and 80%.

Correlation parameters were obtained by minimizing the Root Mean Squared Error (RMSE), $\sqrt{\frac{\sum(S_{L,i,corr}-S_{L,i,data})^2}{n}}$. and are given in Table 5. The reference temperature T_{ref}, the reference pressure P_{ref}, and the reference EGR ratio were arbitrarily fixed at 473 K, 1 bar, and 0%, respectively. Parameters for the reference flame speed (Eq. 9) were determined first and then held constant in the optimization of the parameters relative to the temperature and pressure exponents and the dilution term. The contraints for each parameter are also listed in Table 5. Additional constraints were also imposed for the derivative of flame speeds (positive at over-lean and negative at over-rich conditions) to make sure the generation of realistic S_L at these edge conditions. For conditions where both experimental data and computed flame speeds are available, a weight ratio of 1:1 between the two types of data was kept. Over the whole T, P, φ, and x_d range, the optimized set of correlation parameters exihibits a RMSE of 4.3 cm/s and a coefficient of determination (R^2) of 0.9874 based on 4275 data points.

4.2. Performance on Predicting S_L

Gülder [52] was one of the first to propose an empirical correlation for the laminar flame speeds of gasoline fuels. The mathematical expression adopted for this correlation is given in Eq. 15 and the corresponding parameters are given in Table 6. This correlation has been derived from experimental measurements obtained in a constant volume bomb for isooctane fuel with the addition of ethanol (0-20%). As such, the correlation does not depend on T, P, φ, and x_d but also on the ethanol liquid fraction v.

$$S_L(\varphi, T, P, x_d) = Z \cdot W \cdot \varphi^{\eta} \cdot \exp[-\xi_1(\varphi - \xi_2)^2]\left(\frac{T}{T_0}\right)^{\alpha}\left(\frac{P}{P_0}\right)^{\beta} f(x_d) \tag{15}$$

Later, Yahyaoui [53] adopted the mathematical formulation of Gülder on a ternary mixture representative of commercial gasoline (42.9% isooctane, 13.7% n-heptane, and 43.4% toluene), and developed a correlation for flame speeds based on kinetic modeling using the mechanism by Bounaceur *et al.* [54]. In line with the work of Gülder, some parameters of the correlation depend on the ethanol mole fraction of the fuel. These parameters are given in Table 6 and were obtained from flame speeds computed with an automatically generated

Table 5: Values of the fitted parameters in Eq. (8)–(13) and their constraints.

Category	Parameter	Unit	Value	Constraint
Reference Term	T_{ref}	K	473	positive
	P_{ref}	bar	1	positive
	φ_m		1.0998	positive
	$S_{L,max}$	cm/s	76.6025	positive
	A_1	cm/s	67.1132	positive
	B_1		0.2877	positive
	A_2	cm/s	132.4618	positive
	B_2		0.5586	positive
Temperature Term	φ_α		1.0500	positive
	α_0		1.9835	positive
	α_{A_1}		1.6730	positive
	α_{B_1}		0.4173	positive
	α_{A_2}		141.0423	positive
	α_{B_2}		4.2414	positive
Pressure term	φ_β		5.1563	positive
	β_0		-0.0383	*negative*
	β_2		-0.0117	*negative*
Dilution term	φ_μ		0.9806	positive
	μ_0		3.0861	positive
	μ_2		4.4256	positive
	μ_α		-0.9319	*negative*
	μ_β		0.0538	positive

kinetic model validated on the experimental data of Zhao *et al.* [55] and Jerzembeck *et al.* [56] for the atmospheric pressure and high pressure (10-25 atm) regimes, respectively.

Table 6: Equations and parameters of the existing correlations used for comparison with the correlation developed in the present work.(v and X_{et} are the liquid volume fraction and mole fraction of ethanol, respectively ; x_d is the EGR dilution ratio; ν_{O_2} is the oxygen concentration in the non-fuel portion of the mixture.)

Name	Equations and Parameters		Ref.
Güdler	$S_L(\varphi,T,P,x_d) = Z\cdot W\cdot\varphi^{\eta}\cdot\exp[-\xi_1(\varphi-\xi_2)^2]\left(\frac{T}{T_0}\right)^{\alpha}\left(\frac{P}{P_0}\right)^{\beta} f(x_d)$	cm/s	[52]
	T_0=300 K, P_0=1 bar, W=46.58 cm/s, η=−0.326, ξ_1=4.48, ξ_2=1.075,		
	Z=1+0.07v$^{0.35}$, α=1.56+0.23v$^{0.46}$, β=−0.22, $f(x_d)$=1−2.3x_d		
Yahyaoui	$S_L(\varphi,T,P,x_d) = Z\cdot W\cdot\varphi^{\eta}\cdot\exp[-\xi_1(\varphi-\xi_2)^2]\left(\frac{T}{T_0}\right)^{\alpha}\left(\frac{P}{P_0}\right)^{\beta} f(x_d)$	cm/s	[53]
	T_0=400 K, P_0=1 bar, W=90.31 cm/s, η=2.4269, ξ_1=3.154, ξ_2=0.68157,		
	Z=1+0.14892$X_{et}^{2.4698}$, α=2.236−0.19877$X_{et}^{2.4698}$, β=−0.28327,		
	$f(x_d)$=1−2.4832x_d−0.0020312x_d^2−0.0041743x_d^3		
PRISME	$S_L(\varphi,T,P,\nu_{O_2}) = S_{L,ref}\left(\frac{T}{473K}\right)^{\alpha}\left(\frac{P}{1bar}\right)^{\beta}\left(\frac{\nu_{O_2}}{\nu_{O_2,ref}}\right)^{\gamma}$	cm/s	[25]
	$S_{L,ref}$=73.0208+3.5315(φ−1.1)−138.1265(φ−1.1)^2 cm/s		
	α=1.7495−0.1010(φ−1.1)		
	β=−0.2481+0.0232(φ−1.1)−1.7739(φ−1.1)^2		
	γ=3.4143+0.4252(φ−1.1)		
	ν_{O_2}=n_{O_2}/(n_{air}+$n_{diluent}$)		

Another existing correlation is the one proposed by Di Lorenzo *et al.* [25] based on their experimental measurements. Referred hereafter as the PRISME correlation, its mathemat-

ical formulation and associated parameters are given by Eq. 16.

$$S_L = S_{L,ref}\left(\frac{T}{473K}\right)^{\alpha}\left(\frac{P}{1bar}\right)^{\beta}\left(\frac{\nu_{O_2}}{\nu_{O_2,ref}}\right)^{\gamma} \quad \text{cm/s} \tag{16}$$

$$S_{L,ref} = 73.0208 + 3.5315(\varphi - 1.1) - 138.1265(\varphi - 1.1)^2 \quad \text{cm/s}$$

$$\alpha = 1.7495 - 0.1010(\varphi - 1.1)$$

$$\beta = -0.2481 + 0.0232(\varphi - 1.1) - 1.7739(\varphi - 1.1)^2$$

$$\gamma = 3.4143 + 0.4252(\varphi - 1.1)$$

$$\nu_{O_2} = n_{O_2}/(n_{air} + n_{diluent})$$

4.2.1. Equivalence ratio dependence

Figure 10 compares the predicted laminar flame speeds using the present and the three above-mentioned correlations. One can observe that both Gülder and Yahyaoui correlations overpredict the laminar flame speeds of TRFE at these conditions. At $\varphi \approx 1.1$, the value of S_L estimated by the Gülder correlation is about 17 cm/s higher than the experimental measurement, while the value calculated with the Yahyaoui correlation is only about 10 cm/s faster. The strong overestimation by the Gülder correlation can be rationalized by surprisingly high experimental values used in deriving the correlation parameters. Indeed, the front flame average propagation speed was extracted from the pressure signal and was not extrapolated to the zero-stretch condition, yielding large uncertainties in the reported laminar flame speed. Moreover, the gasoline is emulated by neat isooctane in this correlation, hence introducing another bias. Scaling down the W parameter of the Gülder correlation to match the most recent isooctane flame speed measurements at room temperature and atmospheric pressure gives a value of 27 cm/s at $\varphi = 1.1$ for the conditions of Fig. 10. The deviation observed with the Yayhyaoui correlation may be related to the different TRFE and EGR compositions between their work and the present one. The present correlation and the PRISME correlation are in good agreement with the measurements, which could be expected as they used the experimental data in their training set. Nonetheless, the two correlations exhibit different trends with respect to the equivalence ratio. The PRISME correlation yields a maximum flame speed at a slightly higher equivalence ratio (1.1 vs. 1.07)

and on the fuel-rich branch predicts a slower decay in S_L as the equivalence ratio increases. This latter difference is mostly due to the limited set of data at high equivalence ratio used by Di Lorenzo *et al.* in deriving their correlation, whereas the present work benefited from modeling results, thus an extended equivalence ratio range.

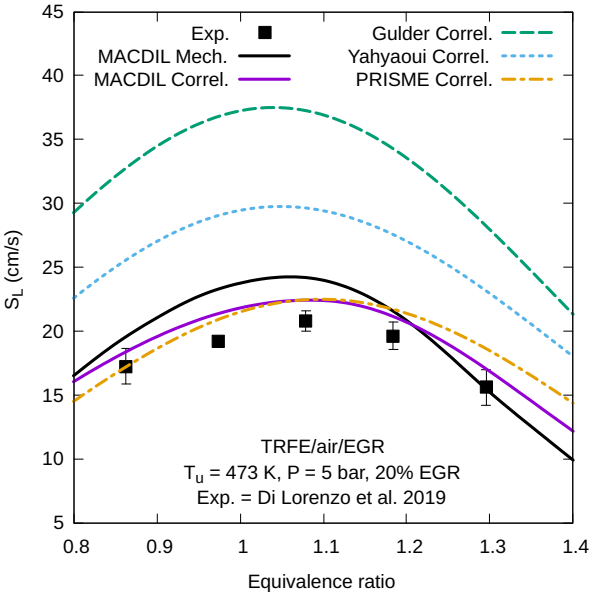

Figure 10: Laminar flame speeds of TRFE/air mixtures at 473 K, 5 bar and diluted in 20% EGR: comparison between experimental data [25], MACDIL Mech. calculations, literature correlations [52, 53, 25] and the present correlation.

4.2.2. Effect of Temperature and Pressure

Figure 11a displays the temperature dependence of the laminar flame speed according to the four correlations as well as the experimental and computed (MACDIL Mech.) S_L without EGR addition for near stoichiometric fuel/air mixtures at atmospheric pressure. The Gülder and the Yahyaoui correlations overestimate the experimental and computed data on the whole temperature range considered (373-973 K), which is consistent with the previous observations of Fig. 10. The PRISME correlation is in excellent agreement with the low-temperature measurements, but its predictions are lower than the MACDIL computations above 600 K. The present correlation, as expected, matches the MACDIL Mech. predictions. To unambiguously compare the temperature dependency in the different correlations, the

data of Fig. 11a are normalized with respect to the value at the reference temperature (473 K) to cancel out other discrepancies related to the reference flame speed expression and displayed in Fig. 11b. At low temperatures (373-473 K) where experimental data are available, the four correlations exhibit a similar trend, all in good agreement with the experimental observations. Deviations start appearing at higher temperatures (> 600 K). The Gülder correlation is the one predicting the slowest increase of S_L with the temperature, followed by the PRISME correlation. The MACDIL and the Yahyaoui's correlations predict nearly identical trends, with a much faster S_L increase than the two others, resulting for both of them at 973 K in a ratio $\frac{S_L}{S_{L,ref}}$ of about 7 which is 30 to 40% higher than the Gülder and PRISME correlation. This higher ratio is consistent with the MACDIL Mech. computations, which have been used for these high temperatures in the training set. This substantial deviation between the two groups of correlation highlights the need for high-temperature data, either from experiments or computations, in deriving accurate empirical correlation since the use of increasing EGR dilution ratios in future combustion engines will increase the in-cylinder pre-combustion temperature.

Figure 12a illustrates the pressure dependence predicted by the four correlations along with the experimental and kinetic modeling trends for a TRFE/air mixture diluted by 20% EGR at $\varphi \approx 1.1$. The Gülder and the Yahyaoui correlations overestimate the laminar flame speed regardless of the pressure, whereas the present and the PRISME correlation predicted values are much closer to the experimental and computed values with only minor differences. Compared with the PRISME correlation, MACDIL correlation predictions are closer to experimental values at low pressure (< 5 bar) and closer to computed values at higher pressures (> 10 bar). Figure 12b displays the normalized flame speed (by the value of S_L at 1 bar) without EGR and with 20% EGR addition. The use of normalized values levels out differences arising from other parameters than the pressure. Except for Yahyaoui's correlation, all correlations match the pressure dependence measured by Di Lorenzo *et al.* without EGR at low pressure. At higher pressure, MACDIL correlation predictions are in between that of Gülder and PRISME and closer to the computed values.

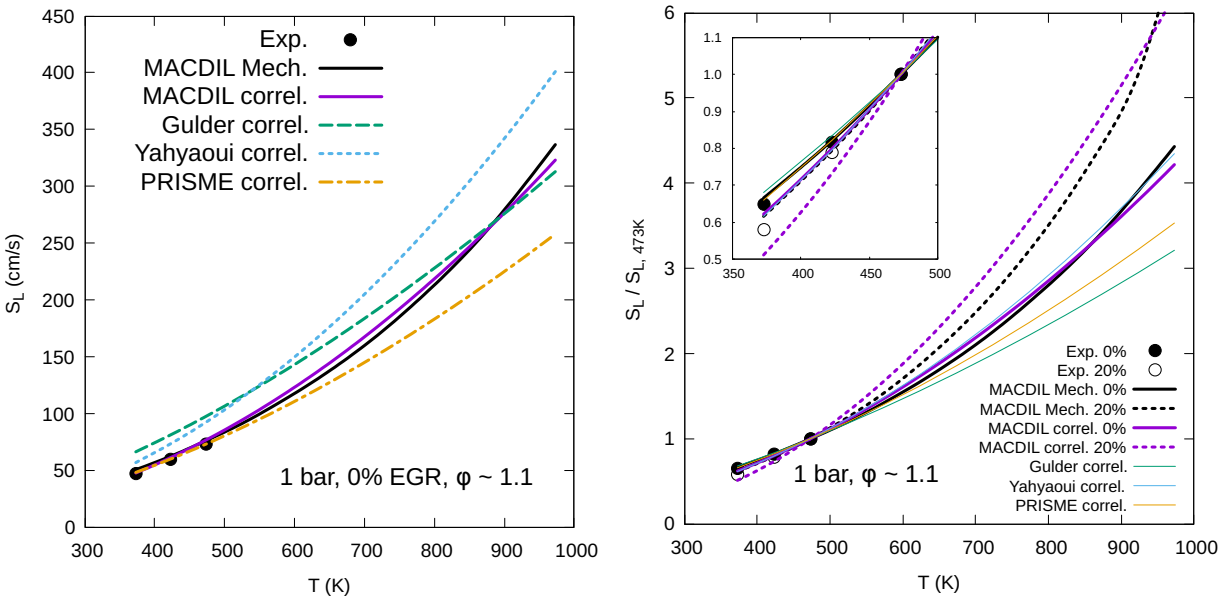

(a) S_L (b) $\frac{S_L}{S_{L,473K}}$

Figure 11: (a) Temperature dependence of the laminar flame speeds of TRFE/air mixtures ($\varphi \approx 1.1$ and 1 bar) and (b) temperature and dilution ratio dependence of the normalized laminar flame speeds of TRFE/air mixtures: comparison between experimental data [25], MACDIL Mech. calculations, literature correlations [52, 53, 25] and the present correlation.

4.2.3. Effect of EGR Addition

The effect of the EGR dilution ratio on the predicted laminar flame speeds by the four correlation is displayed in Fig. 13a at an initial temperature and pressure of 673 K and 5 bar for a near stoichiometric mixture. Such a high temperature was selected to cover a wide range of dilution ratios, although no experimental data are available. A linear dependence with the dilution ratio is observed for the Gülder and the Yahyaoui correlations, resulting in negative laminar flame speeds for dilution ratios above ~40%. Whereas this was expected for the Gülder correlation because of the linear function adopted for $f(x_d)$, such a trend for the Yahyaoui's correlation is more surprising as a cubic polynomial had been used. Nonetheless, the coefficients of the square and cubic terms are relatively small, which may result from the lack of experimental data at high dilution ratios in the training set employed by the authors. The PRISME correlation predicts a dilution ratio dependency

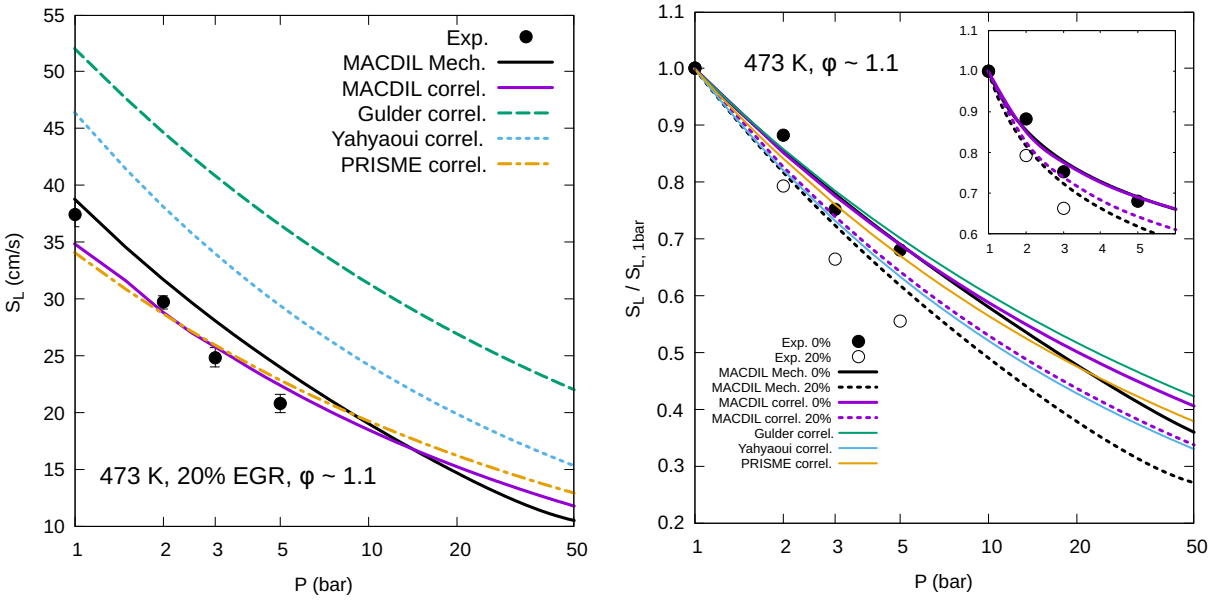

(a) S_L (b) $\frac{S_L}{S_{L,473K}}$

Figure 12: (a) Pressure dependence of the laminar flame speeds of TRFE/air mixtures ($\varphi \approx 1.1$ and 473 K) and (b) pressure and dilution ratio dependence of the normalized laminar flame speeds of TRFE/air mixtures: comparison between experimental data [25], MACDIL Mech. calculations, literature correlations [52, 53, 25] and the present correlation.

similar to the mechanism predictions at the lower dilution ratios (< 0.2) but underestimates the absolute value of flame speeds. At higher dilution ratios (> 0.3), the PRISME correlation underpredicts the inhibiting effect on the laminar flame speed of the diluent and a weaker dilution effect at higher dilutions. The MACDIL correlation exhibits an excellent agreement with the computed values over the whole range of dilution ratio, illustrating the advantage of the dilution term herein proposed (Eq. 12) over the other expressions.

Unlike the Gülder and the Yahyaoui correlations, both the PRISME and the MACDIL correlations consider an equivalence ratio dependence of the dilution term, either through the exponent (Eq. (16)) or the dilution effectiveness parameter μ (Eq. (13)). Figure 13b displays the dilution effectiveness μ at the reference condition (473 K, 1 bar) derived from the experimental data and the MACDIL Mech. calculations as a function of the equivalence ratio. A concave quadratic dependency is unambiguously observed in both cases, rational-

izing the second-order polynomial expression adopted in Eq. 12. The equivalence ratio for which the dilution effectiveness is minimum is obtained at fuel-rich conditions ($\varphi = 1.20$) for experimental data whereas it is around $\varphi = 1.05$ according to the MACDIL Mech.. Nevertheless, the value of this minimum is around 2.6-2.7 in both cases. This figure also shows the equivalent dilution effectiveness μ obtained when Eq. 12 is applied to the PRISME and MACDIL correlations. The PRISME correlation returns a weak linear φ-dependence of the dilution effectiveness, which is consistent with the linear expression adopted for the exponent term of the dilution factor (γ in Eq. 16) but contrary to the experimental observations. Differently, the MACDIL correlation exhibits a quadratic φ-dependence. But the minimum is observed at a lower equivalence ratio ($\varphi = 1.00$) and the predicted dilution effectiveness is consistently higher than computed by the mechanism and experimental values for fuel-rich mixtures. It is noteworthy that the MACDIL correlation (Eq. 13) better captures the equivalence ratio dependence of the dilution term. The discrepancy observed in Figure 13b arises to some extent from the uncertainty in the equivalence ratio associated with the experimental data (as discussed in the previous section), and the resulting attempt of the fitting procedure to concialite both the experimental and modeling sets of data. A better agreement could be achieved by considering only the experimental data or the mechanism predictions.

In addition to equivalence ratio dependency, the MACDIL Mech. and the experimental data indicate that dilution effectiveness could also depend on temperature and pressure and vice versa. Figures 11b and 12b provide S_L evolution with temperature and pressure at both 0% and 20% EGR. Despite the limited temperature and pressure ranges investigated, experimental measurements indicate that the T and P dependence depends on the dilution ratio, which is confirmed by the MACDIL Mech. computations. Therefore, this effect must be included in the final correlation. The dilution ratio dependence of the temperature and pressure dependences can also be formulated as a T and P dependence of the dilution effectiveness, thus preventing the modification of two terms but only one. This was achieved by introducing a simple T and P power dependence in the dilution effectiveness expression, Eq. 12. The fitting process gives for μ_α and μ_β the values -0.9319 and 0.0538, respectively,

implying that increasing the temperature lowers the dilution effectiveness and therefore the reduction of the laminar flame speed whereas an increase in pressure enhances the EGR reduction effect. It can be seen in Fig. 11b that the fitted value of μ_α enables the MACDIL correlation to adequately match the MACDIL Mech. computations over the whole temperature range. However, as displayed in Fig. 12b, the optimized value of μ_β results in an underestimation of the pressure effect on the dilution effectiveness, and then on the flame speed reduction due to the combined effects of the dilution and pressure. Further work is thus necessary to improve the correlation performance and its pressure dependence.

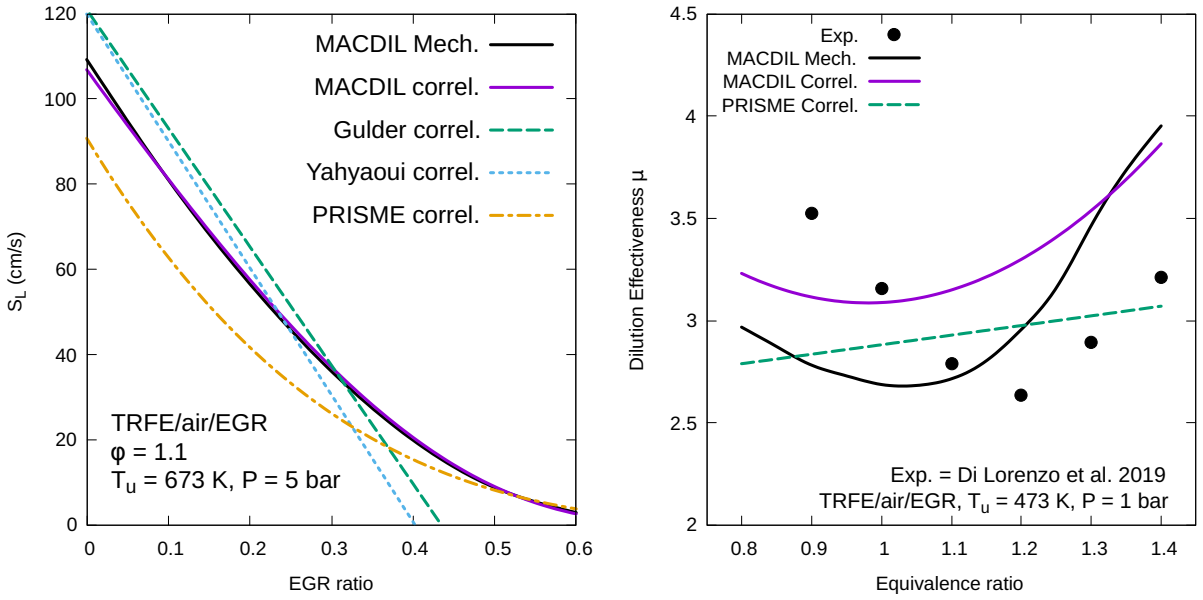

(a) S_L vs. EGR ratio

(b) μ vs. φ

Figure 13: (a) EGR dilution ratio dependence of the laminar flame speeds of TRFE/air mixtures ($\varphi \approx 1.1$, 673 K and 5 bar): comparison between experimental data [25], MACDIL Mech. calculations, literature correlations [52, 53, 25] and the present correlation. (b) Equivalence ratio dependence of the dilution effectiveness μ.

5. Conclusion

The laminar flame speeds of a TRFE surrogate and their dependences on parameters such as equivalence ratio, temperature, pressure, and dilution ratio have been investigated. The limited set of experimental data for TRFE/air EGR mixtures motivated the development of a reduced mechanism, referred to as the MACDIL Mech., that contains 593 species involved in 3698 reactions. It was formulated by compiling state-of-art sub-mechanisms from the literature for each surrogate component (isooctane, n-heptane, toluene, and ethanol), with updates for key reaction rate constants based on recent theoretical and experimental studies. The resulting model was finally reduced using a DRGEP-SA method based on 0-D computations and then successfully validated against the experimental measurements available for the TRFE/air EGR mixtures in the whole [φ, T, P, x_d] domain. The MACDIL Mech. was then used to expand the database of laminar flame speeds for the TRFE surrogate of interest to higher temperatures, pressures, and dilution ratios. This newly expanded database (including both experimental and computed data) was next employed as a training set to derive the optimized coefficients of a new empirical correlation, the MACDIL correlation.

The formulation of this new correlation has been herein devised, with the following new features:

1. the laminar flame speed reference term adopts a dual Gaussian formulation in which the different parameters are related to physical quantities along the S_L-φ curve, thus enabling to capture the different φ-dependences of the fuel-lean and fuel-rich branches;
2. the temperature exponent formulation similarly adopts a two-Gaussian expression, preventing unrealistic overestimations of the laminar flame speeds at over-lean and over-rich conditions, i.e. near the flammability limits;
3. the dilution factor is modeled by an exponential expression, enabling a smooth and non-linear decay of the laminar flame speeds with the dilution ratio and avoiding negative laminar flame speeds in highly diluted conditions by introducing only one new parameter, namely the reduction effectiveness μ;

4. the dilution effectiveness not only depends on the equivalence ratio (φ), the temperature, and pressure (T and P) according to a quadratic expression or a simple exponent dependence but also on the nature of the diluent (the dilution effectiveness of a mixture can be calculated based on a linear mixing rule i.e., $\mu_{mix} = \sum X_i \mu_i$).

The proposed correlation, optimized for the TRFE fuel considered, shows an overall good performance in predicting the dependence of laminar flame speeds to the dilution ratio, equivalence ratio, temperature, and pressure and outperforms previous literature correlations for this fuel or similar fuels. Some improvements of the correlation formulation are still required, especially for the dilution ratio/pressure combined effect on the laminar flame speed. Likewise, the optimization of the correlation parameters would benefit from a larger experimental database, covering a larger T, P, and dilution ratio range.

Nevertheless, the new correlation can be implemented in CFD codes to provide more accurate estimations of laminar flame speeds than existing correlations, and thus improve simulations of turbulent flames at highly EGR-diluted regimes.

Acknowledgment

This work was supported by Agence Nationale de la Recherche [ANR-15-CE22-0014]. The authors thank Dr. Marco Di Lorenzo, Prof. Pierre Brequigny, and Prof. Fabrice Foucher from the PRISME lab for communicating the experimental data. We thank Dr. Giampaolo Maio and Dr. Stephane Chevillard for using MACDIL correlation in CFD simulations. We thank Dr. Lucia Giarracca for using MACDIL Mech. in kinetic modeling.

References

[1] H. Wei, T. Zhu, G. Shu, L. Tan, Y. Wang, Gasoline engine exhaust gas recirculation–a review, Applied energy 99 (2012) 534–544.

[2] G. H. Abd-Alla, Using exhaust gas recirculation in internal combustion engines: a review, Energy Conversion and Management 43 (8) (2002) 1027–1042.

[3] F. Sarikoc, M. Kettner, A. Velji, U. Spicher, A. Krause, A. Elsaesser, Potential of reducing the nox emissions in a spray guided di gasoline engine by stratified exhaust gas recirculation (egr), Tech. rep., SAE Technical Paper (2006).

[4] G. Fontana, E. Galloni, Variable valve timing for fuel economy improvement in a small spark-ignition engine, Applied Energy 86 (1) (2009) 96–105.

[5] Y.-l. Bai, Z. Wang, J.-x. Wang, Part-load characteristics of direct injection spark ignition engine using exhaust gas trap, Applied Energy 87 (8) (2010) 2640–2646.

[6] G. Pilla, L. Francqueville, Stabilization of Highly Diluted Gasoline Direct Injection Engine using Innovative Ignition Systems, SAE International Journal of Engines 7 (4) (2014) 1734–1743. doi:10.4271/2014-01-2598.

[7] T. Poinsot, D. Veynante, Theoretical and numerical combustion, RT Edwards, Inc., 2005.

[8] E. Riber, B. Cuenot, T. Poinsot, Introducing chemical kinetics into large eddy simulation of turbulent reacting flows, in: Computer Aided Chemical Engineering, Vol. 45, Elsevier, 2019, pp. 899–936.

[9] T. W. Ryan, S. S. Lestz, The laminar burning velocity of isooctane, n-heptane, methanol, methane, and propane at elevated temperature and pressures in the presence of a diluent, in: SAE Technical Paper, SAE International, 1980. doi:10.4271/800103.
URL `https://doi.org/10.4271/800103`

[10] M. Metghalchi, J. C. Keck, Burning velocities of mixtures of air with methanol, isooctane, and indolene at high pressure and temperature, Combustion and flame 48 (1982) 191–210.

[11] Ö. L. Gülder, Laminar burning velocities of methanol, ethanol and isooctane-air mixtures, in: Symposium (international) on combustion, Vol. 19, Elsevier, 1982, pp. 275–281.

[12] O. L. Gulder, Correlations of laminar combustion data for alternative s.i. engine fuels, in: SAE Technical Paper, SAE International, 1984. doi:10.4271/841000.
URL `https://doi.org/10.4271/841000`

[13] K. Kumar, J. Freeh, C. Sung, Y. Huang, Laminar flame speeds of preheated iso-octane/o2/n2 and n-heptane/o2/n2 mixtures, Journal of propulsion and power 23 (2) (2007) 428–436.

[14] D. B. Rhodes, J. C. Keck, Laminar burning speed measurements of indolene-air-diluent mixtures at high pressures and temperatures, in: SAE Technical Paper, SAE International, 1985. doi:10.4271/850047.
URL `https://doi.org/10.4271/850047`

[15] I. Z. Syed, Yeliana, A. Mukherjee, J. D. Naber, D. Michalek, Numerical investigation of laminar flame speed of gasoline-ethanol/air mixtures with varying pressure, temperature and dilution, SAE International Journal of Engines 3 (1) (2010) 517–528.

[16] A. Bhattacharya, D. K. Banerjee, D. Mamaikin, A. Datta, M. Wensing, Effects of exhaust gas dilution on the laminar burning velocity of real-world gasoline fuel flame in air, Energy & Fuels 29 (10) (2015) 6768–6779.

[17] A. Clarke, Measurement of laminar burning velocity of air/fuel/diluent mixtures in zero gravity., Ph.D. thesis, University of Oxford (1994).

[18] R. Stone, A. Clarke, P. Beckwith, Correlations for the laminar-burning velocity of methane/diluent/air mixtures obtained in free-fall experiments, Combustion and Flame 114 (3-4) (1998) 546–555.

[19] S. Marshall, S. Taylor, C. Stone, T. Davies, R. Cracknell, Laminar burning velocity measurements of liquid fuels at elevated pressures and temperatures with combustion residuals, Combustion and Flame 158 (10) (2011) 1920–1932.

[20] J. Fu, B. Deng, Y. Wang, J. Yang, D. Zhang, Z. Xu, J. Liu, Numerical study and correlation development on laminar burning velocities of n-butanol, iso-octane and their blends: focusing on diluent and blend ratio effects, Fuel 124 (2014) 102–112.

[21] F. Halter, F. Foucher, L. Landry, C. Mounaïm-Rousselle, Effect of dilution by nitrogen and/or carbon dioxide on methane and iso-octane air flames, Combustion Science and Technology 181 (6) (2009) 813–827.

[22] T. Tahtouh, F. Halter, C. Mounaïm-Rousselle, Laminar premixed flame characteristics of hydrogen blended iso-octane–air–nitrogen mixtures, International Journal of Hydrogen Energy 36 (1) (2011) 985–991.

[23] B. Galmiche, F. Halter, F. Foucher, Effects of high pressure, high temperature and dilution on laminar burning velocities and markstein lengths of iso-octane/air mixtures, Combustion and Flame 159 (11) (2012) 3286–3299.

[24] C. Endouard, F. Halter, C. Chauveau, F. Foucher, Effects of co2, h2o, and exhaust gas recirculation dilution on laminar burning velocities and markstein lengths of iso-octane/air mixtures, Combustion Science and Technology 188 (4-5) (2016) 516–528.

[25] M. D. Lorenzo, P. Brequigny, F. Foucher, C. Mounaïm-Rousselle, Validation of TRF-E as gasoline surrogate through an experimental laminar burning speed investigation, Fuel 253 (2019) 1578–1588. doi:10.1016/j.fuel.2019.05.081.

[26] J. Cho, H. H. Song, Dimensionless parameters determining the effect of dilution on ignition delay of syngas and hydrocarbon fuels, Combustion and Flame 213 (2020) 279–290. doi:10.1016/j.combustflame.2019.11.037.

[27] R. J. Varghese, H. Kolekar, S. Kumar, Demarcation of reaction effects on laminar burning velocities of diluted syngas-air mixtures at elevated temperatures, International Journal of Chemical Kinetics 51 (2) (2019) 95–104. doi:10.1002/kin.21232.

[28] G. Li, M. Zhou, Z. Zhang, J. Liang, H. Ding, Experimental and kinetic studies of the effect of CO2 dilution on laminar premixed n-heptane/air flames, Fuel 227 (2018) 355–366. doi:10.1016/j.fuel.2018.04.116.

[29] J. Santner, F. L. Dryer, Y. Ju, The effects of water dilution on hydrogen, syngas, and ethylene flames at elevated pressure, Proceedings of the Combustion Institute 34 (1) (2013) 719–726.

[30] X. Han, Z. Wang, Y. He, S. Wang, Y. Zhu, A. A. Konnov, Over-rich combustion of CH4, C2H6, and C3H8 +air premixed flames investigated by the heat flux method and kinetic modeling, Combustion and Flame 210 (2019) 339–349. doi:10.1016/j.combustflame.2019.09.009.

[31] M. Metghalchi, J. C. Keck, Laminar burning velocity of propane-air mixtures at high temperature and pressure, Combustion and flame 38 (1980) 143–154.

[32] P. Dirrenberger, H. Le Gall, R. Bounaceur, O. Herbinet, P.-A. Glaude, A. Konnov, F. Battin-Leclerc, Measurements of laminar flame velocity for components of natural gas, Energy & fuels 25 (9) (2011) 3875–3884.

[33] X. Han, Z. Wang, Y. He, S. Wang, Y. Liu, A. A. Konnov, Temperature dependence of the laminar burning velocity for n-heptane and iso-octane/air flames, Fuel 276 (2020) 118007. doi:10.1016/j.fuel.2020.118007.

[34] M. Mehl, W. J. Pitz, C. K. Westbrook, H. J. Curran, Kinetic modeling of gasoline surrogate components and mixtures under engine conditions, Proc. Combust. Inst. 33 (1) (2011) 193–200.

[35] C.-W. Zhou, Y. Li, U. Burke, C. Banyon, K. P. Somers, S. Ding, S. Khan, J. W. Hargis, T. Sikes, O. Mathieu, et al., An experimental and chemical kinetic modeling study of 1,3-butadiene combustion: Ignition delay time and laminar flame speed measurements, Combustion and Flame 197 (2018) 423–438.

[36] Y. Zhang, H. El-Merhubi, B. Lefort, L. Le Moyne, H. J. Curran, A. Kéromnès, Probing the low-temperature chemistry of ethanol via the addition of dimethyl ether, Combustion and Flame 190 (2018) 74–86.

[37] K. Zhang, C. Banyon, J. Bugler, H. J. Curran, A. Rodriguez, O. Herbinet, F. Battin-Leclerc, C. B'Chir, K. A. Heufer, An updated experimental and kinetic modeling study of n-heptane oxidation, Combustion and Flame 172 (2016) 116–135.

[38] N. Atef, G. Kukkadapu, S. Y. Mohamed, M. Al Rashidi, C. Banyon, M. Mehl, K. A. Heufer, E. F. Nasir, A. Alfazazi, A. K. Das, et al., A comprehensive iso-octane combustion model with improved thermochemistry and chemical kinetics, Combustion and Flame 178 (2017) 111–134.

[39] W. Yuan, Y. Li, P. Dagaut, J. Yang, F. Qi, Investigation on the pyrolysis and oxidation of toluene over a wide range conditions. i. flow reactor pyrolysis and jet stirred reactor oxidation, Combustion

and Flame 162 (1) (2015) 3–21.

[40] W. Yuan, Y. Li, P. Dagaut, J. Yang, F. Qi, Investigation on the pyrolysis and oxidation of toluene over a wide range conditions. ii. a comprehensive kinetic modeling study, Combustion and Flame 162 (1) (2015) 22–40.

[41] S.-Z. Xiong, Q. Yao, Z.-R. Li, X.-Y. Li, Reaction of ketenyl radical with hydroxyl radical over C2H2O2 potential energy surface: A theoretical study, Combustion and Flame 161 (4) (2014) 885–897. doi:10.1016/j.combustflame.2013.10.013.

[42] T. V.-T. Mai, P. Raghunath, X. T. Le, L. K. Huynh, P.-C. Nam, M. Lin, Ab initio chemical kinetics for the HCCO+OH reaction, Chemical Physics Letters 592 (J. Chem. Phys. 91 1989) (2014) 175–181. doi:10.1016/j.cplett.2013.11.060.

[43] M. Christensen, A. A. Konnov, Laminar burning velocity of diacetyl+air flames. further assessment of combustion chemistry of ketene, Combust. Flame 178 (2017) 97–110.

[44] A. S. Savchenkova, A. S. Semenikhin, I. V. Chechet, S. G. Matveev, A. M. Mebel, A. A. Konnov, Revisiting diacetyl and acetic acid flames: The role of the ketene+OH reaction, Combustion and Flame 218 (2020) 28–41. doi:10.1016/j.combustflame.2020.04.021.

[45] B. Xu, J. Garrec, A. Nicolle, M. Matrat, L. Catoire, Temperature and pressure dependent rate coefficients for the reaction of ketene with hydroxyl radical, The Journal of Physical Chemistry A 123 (13) (2019) 2483–2496.

[46] A. S. Savchenkova, A. S. Semenikhin, I. V. Chechet, S. G. Matveev, A. A. Konnov, A. M. Mebel, Mechanism and rate constants of the ch2+ch2co reactions in triplet and singlet states: A theoretical study, J. Comput. Chem. (2018).

[47] A. Semenikhin, E. Shubina, A. Savchenkova, I. Chechet, S. Matveev, A. Konnov, A. Mebel, Mechanism and rate constants of the $CH_3 + CH_2CO$ reaction: A theoretical study, Int. J. Chem. Kinet. 50 (4) (2018) 273–284.

[48] R. Kee, F. Rupley, J. Miller, M. Coltrin, J. Grcar, E. Meeks, H. Moffat, A. Lutz, G. Dixon-Lewis, M. Smooke, et al., CHEMKIN-PRO 15131, Reaction Design, San Diego, CA (2013).

[49] R. J. Kee, J. F. Grcar, M. D. Smooke, J. A. Miller, E. Meeks, PREMIX: a Fortran program for modeling steady laminar one-dimensional premixed flames, Sandia National Laboratories Report (SAND85-8249) (1985).

[50] O. Mannaa, M. S. Mansour, W. L. Roberts, S. H. Chung, Laminar burning velocities at elevated pressures for gasoline and gasoline surrogates associated with ron, Combustion and Flame 162 (6) (2015) 2311–2321.

[51] O. A. Mannaa, M. S. Mansour, W. L. Roberts, S. H. Chung, Influence of ethanol and exhaust gas recirculation on laminar burning behaviors of fuels for advanced combustion engines (face-c) gasoline

and its surrogate, Energy & fuels 31 (12) (2017) 14104–14115.

[52] Ö. L. Gülder, Correlations of laminar combustion data for alternative si engine fuels, Tech. rep., SAE Technical Paper (1984).

[53] M. Yahyaoui, Private communication, Tech. rep., IFPEN Internal Report (2010).

[54] R. Bounaceur, O. Herbinet, R. Fournet, P.-A. Glaude, F. Battin-Leclerc, A. P. da Cruz, M. Yahyaoui, K. Truffin, G. Moreac, Modeling the laminar flame speed of natural gas and gasoline surrogates, Tech. rep., SAE Technical Paper (2010).

[55] Z. Zhao, J. P. Conley, A. Kazakov, F. L. Dryer, Burning velocities of real gasoline fuel at 353 k and 500 k, SAE transactions (2003) 2624–2629.

[56] S. Jerzembeck, N. Peters, P. Pepiot-Desjardins, H. Pitsch, Laminar burning velocities at high pressure for primary reference fuels and gasoline: Experimental and numerical investigation, Combustion and Flame 156 (2) (2009) 292–301.

Semi-Detailed Mechanism

- MACDIL Mech.
- 593 species, 3698 reactions
- Validated on Exp. data

+ Exp. from Di Lorenzo et al.

SL Correlation for TRFE

- 4275 dpts: 373-973 K, 1-50 bar, φ = 0.4-2.0, 0 – 80% EGR
- RMSE = 4.3 cm/s, R^2 = 0.9874

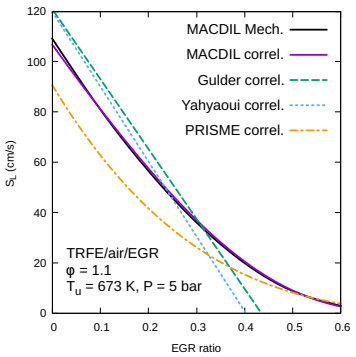

S_L Database for TRFE Gasoline Surrogate

Novel Formulas for Laminar Flame Speeds Correlation

$$S_L(\varphi,T,P,x_d) = S_{L,ref}\left(\frac{T}{T_{ref}}\right)^{\alpha}\left(\frac{P}{P_{ref}}\right)^{\beta} f(x_d)$$

Reference Flame Speed & Temperature Exponent

- Gaussian function + step function
- Better fit at over-rich and over-lean conditions
- Avoid unrealistic SL near flammability limits

$$S_{L,ref}(\varphi) = \begin{cases} A_1 \exp\left[-\frac{1}{2}\left(\frac{\varphi-\varphi_m}{B_1}\right)^2\right] + (S_{L,max} - A_1), & \varphi > \varphi_m \\ A_2 \exp\left[-\frac{1}{2}\left(\frac{\varphi-\varphi_m}{B_2}\right)^2\right] + (S_{L,max} - A_2), & \varphi \le \varphi_m \end{cases}$$

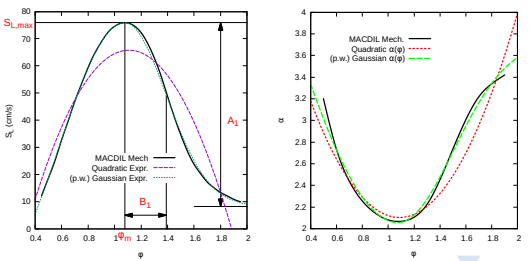

$$\alpha(\varphi) = \begin{cases} \alpha_0 + \alpha_{A_1} - \alpha_{A_1}\exp\left[-\frac{1}{2}\left(\frac{\varphi-\varphi_\alpha}{\alpha_{B_1}}\right)^2\right], & \varphi > \varphi_\alpha \\ \alpha_0 + \alpha_{A_2} - \alpha_{A_2}\exp\left[-\frac{1}{2}\left(\frac{\varphi-\varphi_\alpha}{\alpha_{B_2}}\right)^2\right], & \varphi \le \varphi_\alpha \end{cases}$$

$$\beta(\varphi) = \beta_0 + \beta_2(\varphi - \varphi_\beta)^2$$

Dilution Factor

- Exponential formula for non-linear dilution effect
- Better fit at highly-diluted conditions
- Only 1 parameter needed: μ

$$f(x_d) = \exp\left(-\frac{\mu x_d}{1-x_d}\right)$$

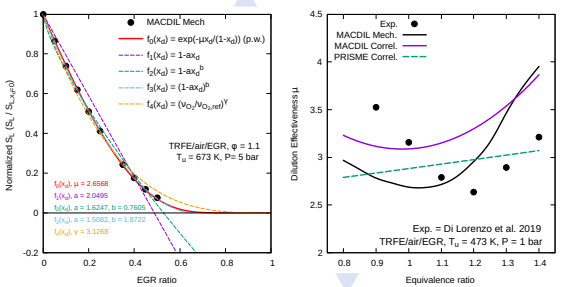

$$\mu(\varphi,T,P) = \left(\mu_0 + \mu_2(\varphi-\varphi_\mu)^2\right)\left(\frac{T}{T_{ref}}\right)^{\mu_\alpha}\left(\frac{P}{P_{ref}}\right)^{\mu_\beta}$$

Dilution Effectiveness (μ)

- Diluent-specific
- Dependent on Equivalence ratio
- Follow linear blending rule

$$\mu_{mix} = \sum_i X_i \mu_i$$